Wheat inositol pyrophosphate kinase (TaVIH2-3B) interacts with Fasciclin-like arabinogalactan (FLA6) protein and alters the plant cell-wall composition

Mandeep Kaur[1,2,#], Anuj Shukla[1,#], Swati Kanwar[1], Vishnu Shukla[1], Gazaldeep Kaur[1], Shivani Sharma[1], Anil Kumar[1], Sipla Aggarwal[1], Kaushal K Bhati[1], Pratima Pandey[3], Koushik Mazumder[1], Vikas Rishi[1] and Ajay K Pandey[1,*]

Author affiliations

National Agri-Food Biotechnology Institute (Department of Biotechnology), Sector 81, Knowledge City, S.A.S. Nagar, Mohali-140306, Punjab, India.

[2]Department of Biotechnology, Panjab University, Punjab, India.

[3]Department of Biological Sciences, Indian Institute of Education and Research, Mohali 140306.

# These authors contributed equally to this work

*Corresponding author:

Dr. Ajay K Pandey, Scientist-E

Email: pandeyak@nabi.res.in; pandeyak1974@gmail.com

ORCID iD: https://orcid.org/0000-0003-1064-139X

Running title: Inositol pyrophosphate kinase involve in composition of plant cell-wall

Abstract

Inositol pyrophosphates (PPx□InsPs) are of key interest, since they are known to participate in multiple physiological processes from lower eukaryotes to humans. However, limited knowledge is available for their role in plants and especially in crops. In this study, two diphosphoinositol pentakisphosphate kinase PPIP5K wheat homologs, *TaVIH1* and *TaVIH2* were identified and characterized for their spatio-temporal expression along with their physiological functions. The biochemical assay demonstrated the presence of active VIH-kinase domains as evident from the $InsP_6$ phosphorylation activity. The yeast complementation assays showed differential function, where only *TaVIH2-3B* was capable of rescuing the growth defects of yeast *vip1Δ* genotype. Reporter assays with TaVIH2-promoter in *Arabidopsis* displayed strong GUS expression in response to dehydration stress and Pi-starvation with similar observations noted at the transcriptional level. In an attempt to identify VIH2 function, a yeast two hybrid screen of wheat library resulted in the identification of multiple interacting proteins primarily associated with cell-wall. One such interactor of wheat VIH2-3B was identified to be a Fasciclin-like arabinogalactan protein (FLA6) that was confirmed by pull-down assay. Systematic analysis of transgenic *Arabidopsis* overexpressing TaVIH2-3B protein showed robust growth and enhanced relative water content when compared to controls. Biochemical analysis of their cell-wall components in the shoots resulted in increased accumulation of polysaccharides such as cellulose, arabinogalactan and arabinoxylan, whereas *Atvih2-3* mutant showed decrease in some of these components. Overall, our results provide novel insight into the functional role of inositol pyrophosphate kinases that modulate cell-wall components so as to provide tolerance towards the dehydration stress.

Keywords: Inositol pyrophosphate kinase, wheat, drought stress, phytic acid, dehydration, Pi-starvation,

Introduction

In plant seeds, the most abundant inositol polyphosphate referred as, Inositol hexa*kis*phosphate (Phytic acid, $InsP_6$) is the primary source of stored phosphorus (P) which is utilized by the plants to draw energy during the process of seed germination. Although in cereal crops it is primarily considered as a major antinutrient because of its ability to chelate major micronutrients (Fe, Zn) yet, $InsP_6$ plays diverse roles in plant development and other signalling processes[1]. Cereal crops with lower levels of $InsP_6$ is considered as an important trait, but it also acts as a precursor for the higher anionic derivatives referred as inositol pyrophosphates (PP-InsPx). These diphospho-inositol polyphosphates including diphosphoinositol pentakisphosphate (PP-$InsP_5$) and bisdiphosphoinositol tetrakisphosphate [(PP) $_2InsP_4$] are the most recent members of the inositol phosphate family and have emerged as distinct molecules possessing the most packed arrays of phosphates around an inositol ring[2]. The inositol pyrophosphates have been attributed a discrete property of being energy rich molecules as the free energy of hydrolysis for the pyrophosphate moiety is similar to high-energy bond found in ATP[3]. This structurally and functionally diverse class of inositol phosphates are now well characterized in non-plant eukaryotes, yet their existence and possible role in plants is meagre[4].

The roles of high energy pyrophosphates such as $InsP_7$ and $InsP_8$ are largely unexplored, but their functional studies in humans cell lines and yeast suggest their involvement in regulating telomere length, aberrant DNA recombination, endocytic trafficking, vacuolar morphology, phosphate homeostasis, gene expression, protein phosphorylation and other cellular functions[5-9]. Studies in *Dictyostelium*, yeast, humans and plants suggested the presence of such highly charged anionic forms at a very low concentration[4,5]. These inositol pyrophosphates are predominantly synthesized by two different classes of enzymes that exhibit catalytic activity towards different positions on the six-C inositol ring. The first class $InsP_6$- kinases (IP6Ks) place a phosphate group at 5th position of the fully phosphorylated ring of $InsP_6$ to form 5PP-$InsP_5$ ie 5-$InsP_7$ [10,11]and two isomers of $InsP_8$: 1/3,5PP-$InsP_5$ and 5PPP-$InsP_5$ [12].The second lineage of enzymes: diphosphoinositol pentakisphosphate kinases (PPIP5Ks) phosphorylate the 1st position of $InsP_6$ synthesizing 1PP-$InsP_5$[13,14,15]. These enzymes also catalyse the conversion of 5PP-$InsP_5$ to 1,5$[PP]_2IP_4$ ie $InsP_8$ which was first demonstrated in mammalian cells[3]. The past two decades showed up the discovery of three isoforms of $InsP_6$-kinases: IP6K1, IP6K2 and IP6K3 in mammals and a

single $InsP_6$ kinase in yeast called Kcs1 along with two PP-IP_5-kinases: PP-IP5K1 and PP-IP5K2 in mammals and single in yeast called as VIP1[14,15].

Recently two plant genes encoding for inositol pyrophosphate kinases (PPIP5Ks) were identified from *Arabidopsis*[16]. Their work described the identification and expression characterization of two kinases without providing evidence for the probable functions. Subsequently, in the same year, functional characterization of *AtVIH2* was performed wherein, the authors proposed the role of VIH2 in plant defense that is dependent on the levels of jasmonate[17]. Studies demonstrate that VIH proteins are conserved throughout the eukaryotic taxa in having a dual domain structure with relevance to the inositol signalling enzyme: a "rim-K" or ATP-grasp superfamily domain at the N-terminal and a C-terminal histidine acid-phosphatase (HAPs) or phytase domain [15]. Irrespective of highly conserved domain architecture, the functions of inositol pyrophosphate kinases during plant growth and stress adaptations remain unexplored. Various experiments have implicated the binding of plant SPX domains to InsP6 and inositol pyrophosphates that throws light on possible influence during phosphate homeostasis by PP-InsPs[18]. Furthermore, inositol pyrophosphates also influence inorganic polyphosphates (polyP) synthesis, which might act as a reservoir for different inositol phosphates and buffering of cellular free phosphate (Pi) levels that are ultimately necessary to generate ATP and inositol pyrophosphate [8,19,20]. A recent study has confirmed the coordinated molecular interplay amongst inorganic polyP, ATP and Ins-PPs which plays a critical role in regulating phosphate homeostasis in eukaryotic cells[21]. Function of the protein could also be studied in context to its interacting partners. In yeast, histone H3/H4 chaperone Asf1p is known to interact with the VIP1 (VIH) protein, thereby, suggesting this interaction important for transcription elongation [22]. Such comprehensive interaction studies for VIH protein are missing in plants that could provide new insight into their functional roles.

Previously, it was identified that that barley contains inositol phosphate molecules more polar than $InsP_6$[23]. Wheat is an important source of nutrition in the developing countries and has been a target crop for multiple trait enhancement. Therefore, it is encouraging to investigate the functional importance of inositol pyrophosphate kinase genes especially when the developing grains accumulate high amounts of $InsP_6$ that could be one of the substrates for VIH protein activity. In the current study, we have cloned two VIH genes from hexaploid wheat and detailed expression characterization was performed. GUS-reporter based assays of wheat VIH promoters were performed in *Arabidopsis* that indicate their function during dehydration and Pi-starvation. Our data suggest that wheat

VIH proteins are catalytically active and VIH2-3B were able to complement the growth defects associated with yeast *vip1* null mutation. At the protein level wheat VIH2-3B interacts with Fasciclin-like arabinogalactan protein (FLA6) and other multiple cell-wall related proteins. Overexpression studies of *TaVIH2-3B* in *Arabidopsis* showed better relative water content in leaves and changes in the composition of plant cell-wall. A significant change in the content of arabinogalactan, arabinoxylans and cellulose was observed that was in contrast to the *Atvih2-3* cell-wall composition. Taken together, our study provides novel insight for the possible function of plant VIH protein in cell-wall reinforcement.

Results

Conserved domain-architecture of plant VIH proteins

To identify the wheat VIH genes, previously reported *Arabidopsis* VIH sequences (At3g01310, At5g10570) were used as a query that resulted in the identification of six potential wheat VIH-like sequences. The identified transcripts included three homoeologs each for *TaVIH1* and *TaVIH2* which were mapped on chromosome number 4 and 3 respectively. *In-silico* analysis of the peptide sequences show variation in amino acid length that varied in 1000-1060 amino acids with *TaVIH1-4B* having the shortest length of 1012 aa (Supplementary Table S1). The Kyte-Doolittle hydropathy plots indicated that wheat VIH proteins do not contain any potential transmembrane regions (Supplementary Figure S1).

The analysis clustered plant VIH homologs together with TaVIH proteins close to their *Brachypodium* counterparts in the monocot specific clade (Figure 1A). Amino acid sequence alignment of wheat VIH protein sequences suggested the presence of conserved dual domain architecture of PPIP5K/Vip1 family with typical N-terminal ATP-grasp kinase domain that has the inositol pyrophosphate kinase activity and a C-terminal histidine acid phosphatase domain (Figure 1B). The catalytic aspartic acid residue, a key residue required for the kinase activity as well as the phosphorylated serine residue were found to be conserved in both the wheat VIH proteins as suggested earlier[16]. The amino acid sequences exhibited 72% identity amongst two wheat VIH proteins, while TaVIH1 is closest wheat ortholog of AtVIH proteins (78% identity). TaVIH2 have70% and 70.6% identity to AtVIH1 and AtVIH2 respectively. Both TaVIH proteins showed a percentage identity of 33% to yeast VIP protein. The homoeologs of *TaVIH1* were found to have different number of exons with

TaVIH2 gene arising from different genomes having as many as 30 exons with a genome size of 29-34 kb (Figure 1C).

Spatial-temporal expression characterization of VIH genes in wheat tissue

Transcript accumulation of *TaVIH* genes was studied in different tissues of a 14 DAA plant including root, stem, leaf and flag leaf. The results showed similar expression profiles for both genes with highest expression in leaf tissue followed by flag leaf, root and with least expression in stem (Figure 2A&B). The transcript accumulation of *TaVIH1* was 1.5-fold higher than *TaVIH2* in all the tissues investigated. These findings suggest that both VIH genes are preferentially expressed in leaf. Highest expression of both VIH genes was observed at the late stages of grain filling with maximum transcript accumulation at 28 DAA stage (Figure 2C). Interestingly, the pattern of gene expression remained same, wherein *TaVIH1* showed 3-fold higher expression in comparison to *TaVIH2* at all stages.

The expression profile in different grain tissues revealed a high expression of *TaVIH* genes in the aleurone layer which is ~ 4-fold higher than in endosperm (Figure 2D). Our results indicate almost similar levels of transcript accumulation in the remaining grain tissues *viz*. embryo, glumes and rachis; suggesting a ubiquitous expression in these tissues. In general, expression levels of *TaVIH1* was more than *TaVIH2* during all stages of wheat development (Figure 2E). Overall, our expression analysis using ExpVIP database conducted in different tissues showed high expression for *TaVIH1* transcripts from B and D genomes. *TaVIH2* did not show any significant expression in majority of tissues, however a weak expression was found in spikes (Supplementary Figure S2A). Expression of wheat VIH was also studied in abiotic stress conditions wherein, they showed differential expression patterns. Under phosphate (Pi) starvation, a strong induction of *TaVIH2* transcripts was noted in roots as well as shoots; whereas *TaVIH1* was downregulated. Heat and drought stress seemed to down regulate the expression of *TaVIH1* in a time dependent manner (Supplementary Figure S2B). Under biotic stress imposed by both stripe rust and powdery mildew pathogens, a late stage of infection at 72 hrs showed significant increase in transcripts of both *VIH* genes (Supplementary Figure S2C). Varying expression patterns displayed by *TaVIH* genes in different conditions suggest their role in different development processes and stress response.

Wheat VIH proteins display kinase activity and complement yeast mutant differentially

The homology modelled structure for VIH proteins, based on hPPIP5K2 (PDB ID: 3T9C) predicted two antiparallel β-sheets to co-ordinate the nucleotide analog AMP-PNP (Figure

3A). Additionally, like human and *Arabidopsis* homologs, wheat VIH proteins also appear to use only arginine and lysine residues in the inositol phosphate binding pocket, with an exception of a serine residue (Figure 3B). To explore the evolutionary conserved kinase activity of wheat VIH proteins biochemical activity was checked using respective kinase domain (VIH-KD) of wheat VIH1 and VIH2 proteins. The kinase activity was tested by using two different concentrations of the $InsP_6$ (40 µM and 80 µM). The relative luminescence units (RLU) recorded for TaVIH1-KD at both $InsP_6$ concentrations showed > 6-fold higher activity with respect to control (Figure 3C). Similar results were obtained with TaVIH2-KD, indicating the saturation of TaVIH-KD at 40 µM $InsP_6$ concentration as an increase in substrate concentration did not bring any significant change in kinase activity. However, lowering down the protein concentration by 1/5 brought 4-fold reduction in kinase activity of both proteins. As a result of this luminescence-based kinase assay, we confirmed that both TaVIH-KD proteins are functionally active and use $InsP_6$ as their substrate.

In order to carry out a yeast complementation assay for wheat VIH genes, the full length ORF of both *TaVIH* was cloned into yeast expression vector pYES2. The growth assay was performed on SD-Ura plates supplemented with 0, 2.5 and 5 mM 6-azuracil. The wild type strain BY4741 showed an unrestricted growth phenotype under all three experimental conditions tested. The *vip1Δ* transformed with empty pYES2 vector showed growth sensitivity at 2.5 and 5mM concentrations (Figure 3D). To our surprise, the mutant strain transformed with pYES2-TaVIH1 could not revive growth on plates supplemented with 6-Azauracil. Whereas, the one carrying pYES2-TaVIH2 expression cassette was able to rescue the growth phenotype of *vip1Δ* strain. The results suggested that *TaVIH2* derived from the B genome is capable of complementing the growth defects of *vip1Δ* strain in synthetic media supplemented with 6-Azauracil.

Wheat VIHs respond to dehydration stress and Pi starvation

In an attempt to understand the transcriptional regulation of wheat VIH genes, promoters of wheat VIH1 and VIH2 were scanned for the presence of *cis*-elements. Promoters oaf ~1612 and ~1820 bp region for TaVIH1 and TaVIH2 upstream of the start codon were cloned and sequenced. Comparing these upstream promoters on PLANTCARE database revealed the presence of various hormone and abiotic stress responsive cis elements (Figure 4A). Apart from the information obtained from *in silico* search, few putative motifs responsible for abiotic stress response were also identified. The hormone responsive *cis* acting elements included WRKY71OS, ABRELATED1 and MYC for ABA response, ACGTATERD1 for

response to dehydration. The presence of these elements suggests that wheat *VIH* could be regulated by the respective stresses. Additionally, the promoter of *VIH2* contains a P1BS motif (GNATATNC) and three PHO4 binding sites in promoter regions of both *TaVIH* genes (Supplementary Figure S3A).

To investigate the possible in-planta roles of wheat VIH genes, the VIH promoters:GUS (pVIH1/2:GUS) fusion constructs were transformed in *Arabidopsis* (Col0). The GUS expression was tested by subjecting the two weeks old seedlings to dehydration, drought, ABA, GA_3 and Pi-starvation. To our surprise, none of these stresses were able to induce the *TaVIH1* promoter. In contrast, *TaVIH2* promoter responds strongly only to dehydration and Pi starvation (Figure 4B). Significant increase for GUS activity in *pVIH2:GUS* lines indicates the ability of this promoter to drive GUS reporter gene expression. A strong GUS expression was visualized along the midvein and leaf base of the seedlings subjected to Pi-stress. A weak expression of VIH2 promoter was also observed in presence of ABA and GA_3 (Figure 4B). Control (Empty vector-EV) transformants showed no visible GUS staining (data not shown) Based on our reporter assays, it is evident that TaVIH2 may be involved during dehydration and Pi starvation responses.

To confirm the above observations, expression of wheat *VIH* genes were also performed in root and shoot tissues of wheat seedlings subjected to Pi-starvation for the 5, 10, 15 and 20 days. As an experimental control, we confirmed positive expression of phosphate starvation response related marker genes PHR1, IPS1 and phosphate transporters, validating fidelity of phosphate starvation condition[24]. The differential expression response was observed in control plants at different time points, suggesting the role of wheat *VIH* genes in growth time course. An obvious contrasting response was observed for both genes in Pi-limiting condition. The expression profile of *TaVIH1* under starvation portrayed down-regulation of the gene in roots as well as shoots, except for 20-day shoots sample (Figure 5A). Whereas, *TaVIH2* transcript showed enhanced expression in all four studied time points, with maximum induction of 8-fold in roots at 20 days. In shoot tissues, the maximal induction of 12-fold was obtained at 15 days. RNA-seq information from wheat seedlings subjected to -Pi condition that was used for calculating the RPKM showed transcript abundance of *TaVIH2* in shoots as compared to roots under Pi stress (Supplementary Figure S3B and Table S2). The level of transcript expression of *TaVIH1* was notably down-regulated by 2.5-fold in shoot tissues.

Expression studies were also performed for VIH genes subjected to dehydration stress. No apparent increase in expression of VIH1 was observed in roots, but downregulation

in shoots was noted. On the contrary, *TaVIH2* showed a slight up-regulation in drought treated shoots samples (Figure 5B). As inferred from the expression studies, the change in VIH transcript levels confirms that expression of *TaVIH2* is modulated by both drought condition and Pi-starvation.

Yeast two-hybrid screening identifies Fasciclin-like arabinogalactan protein (FLA) as a VIH2 interactor

Previously, no functional clues have been provided for plant VIH proteins except for their involvement in the plant-pathogen interaction[17]. To investigate the additional role for plant VIH proteins, yeast two-hybrid (Y2H) screening was performed using TaVIH2-3B as bait against wheat cDNA library. Protein expression of bait (VIH2) in the yeast cells was confirmed by Western blot analysis (Supplementary Figure S4A). Two pooled wheat cDNA libraries were prepared for the screening process (Supplementary Figure S4B). Our screening resulted in the identification of 89 putative yeast colonies with a mating efficiency of 3.8 % (Supplementary Figure S4C and D). Subsequent stringent screening of the colonies lead to the identification of ~52 putative interactors. Upon sequencing of the ORFs, clones appearing more than twice were considered for further studies. A careful analysis lead to shortlisting eleven strong potential interactors with predicted diverse function as listed in Table 1. Interestingly, enrichment of multiple (3-6) independent cDNAs encoding for cell-wall related proteins were observed. Amongst these 17 colonies represented genes encoding for Fasciclin-like arabinogalactan protein, glycosyl-transferases and glycine-rich cell-wall like structural proteins. This suggests that VIH2 primarily interacts with cell-wall related proteins and could be involved in providing mechanical strength and related agronomical traits.

One of the interacting clones that appeared quite frequently (six times), encoded for Fasciclin-like arabinogalactan protein (FLA). The FLA proteins are known to respond against different stress conditions and are involved in plant growth and development[25]. Therefore, to confirm this interaction, full-length cloning of wheat cDNA (1.2 kb) for *TaFLA6* was done in pGADT7. The growth of the co-transformed (TaFLA6:AD+TaVIH2:BD) yeast colonies on -His/-Leu/-Trp (AbA) media confirmed the full-length interaction of these two proteins (Figure 6A). To further validate the interaction, pull-down assays were performed and the interaction was confirmed by performing immunoblotting. Thus, pull-down assay confirmed that TaVIH2 and TaFLA6 interacts at the protein level and hence, they might be involved in similar molecular function (Figure 6B).

Localization of FLA6 and its differential expression in wheat tissue

Localization experiments were performed using HA tagged FLA6 in *S. cerevisiae* strains. Based on the localization studies we concluded that FLA6 was present on the yeast plasma membrane (Figure 6C). Similarly, localization of VIH2 was also performed in the *S. cerevisiae* strain using c-MYC tagged VIH2. The c-MYC tagged VIH2 showed localization near the rim of the plasma membrane that was cytoplasmic. These evidences point that the GPI anchored cytoplasmic domain of FLA6 is responsible for its interaction with the VIH2 protein. Wheat FLA6 encodes a 367 aa protein containing FAS-like arabinogalactan protein with presence of typical TMD and glycophosphatidyl-inositol (GPI) domain. The protein hydropathy plot identified a hydrophobic region near GPI region at C-termini (Figure 6D). GPI domain is important for the proper anchoring of the cell surface targeted protein[26,27].

Transcript expression response for key components of cell-wall reinforcement that includes *TaFLA6, TaGT* and *TaXat1* was also carried out during drought condition. Our results indicated *TaFLA6, TaGT* and *TaXat1* are significantly upregulated in the shoot and root tissue subjected to drought stress (Figure 7A). Similar observation was also obtained through exVIP gene expression analysis (Supplementary S5). Differential expression pattern for all the above genes was observed during grain development with significant increase in transcript during the seed maturation (Figure 7B). Wheat FLA6 transcript abundance increases (~2-3 fold) during grain maturation. These data indicated that *TaFLA6* and *TaGT/Xat* show transcriptional changes during desiccation that is a prerequisite step for grain maturation. Important interacting clones including *TaGT* and *TaXat* were also expressed in other tissue including developing roots and grain (Figure 7C). Specifically, our data suggested that wheat *VIH2* and *FLA6* are co-expressed under dehydration stress and the proteins interact physically.

Overexpression of TaVIH2-3B in Arabidopsis leads to structural changes in cell-wall

Multiple interacting clones of the VIH2 were identified as cell-wall structural proteins potentially involved in its biosynthesis or wall plasticity. One of the VIH interactors, GPI anchored protein (FLA) was linked with the plant cell-wall composition and morphogenesis[28]. This led to the speculation for the possible role of plant VIH proteins in modulating the cell-wall structure development. Therefore, we developed *Arabidopsis* overexpressing lines for TaVIH2-3B. After preliminary screening, the lines with the highest expression for TaVIH2-3B in T3 and T4 lines were used in further analysis (Figure 8A).

Transgenic *Arabidopsis* show robust growth and enhanced branching with an overall increase in length of main shoot axis for all the transgenic lines (Figure 8B). Assays to measure relative water content after dehydration of transgenic and non-transgenic plants suggested significantly higher retention of moisture in overexpressed lines as compared to controls plants. This retention of water was significant in leaves of transgenic plants subjected to 19- and 24-days post dehydration stress.

To check if wheat VIH could influence cell-wall composition changes, the cell-wall of wild type, transgenic lines overexpressing TaVIH2-3B were extracted using Na_2CO_3 and NaOH (Supplementary Figure S6). This was done to generate fractions to use for the extraction of arabinogalactans (AG: arabinose & galactose) and arabinoxylan (AX: arabinose & xylans), whereas the unextracted fraction mainly contain cellulose. Gas chromatography-mass spectrometry (GC-MS) analysis was performed to analyse the constituent monosaccharide as alditol acetate derivative. Since such chemical analysis requires relatively large amounts of samples, pools from 3-5 independent plants of the respective lines expressing wheat VIH2 were used for chemical analysis. Extraction resulted in almost similar amount of yields from control and transgenic plants. The biological replicates of transgenic *Arabidopsis* showed maximum fold accumulation of cellulose that varied from 3.5 to 5.8-fold increase as compared to control plants. Similarly, AX and AG content increased in range of 1.8- 2.2 and 1.47- 1.5-fold in overexpression lines as compared to controls (Supplementary Figure S7 and Table S3). AtVIH2 is the closest homolog for wheat TaVIH2. Therefore, to verify the involvement of AtVIH2 in cell composition the total AX, AG and cellulose content was measured in the shoots of *Atvih2-3* mutant line[17]. Our analysis showed a significant reduction of the AG and AX content in the mutant line, whereas no reduction was observed for cellulose. (Figure 9). Surprisingly, a slight increase in the levels of cellulose was observed in *Atvih2-3* mutant as compared to Col-0. Altogether, our data demonstrate that overexpression of plant VIH in *Arabidopsis* may provide mechanical strength by modulation of the compositional change in the cell-wall biosynthesis related sugars.

Discussion

Most of the cereal plants contain high amount of $InsP_6$ that act as one of the substrates for plant VIH proteins for the biosynthesis of higher forms of PP-InsPx. To offer the functional clues of plant VIH proteins more in-depth studies need to be performed. In this work, we showed that overexpression of TaVIH2 in *Arabidopsis* could enhance growth and provide tolerance to the dehydration stress. This study also identified FLA6 as one of the interactors

of TaVIH2 as evident from our biochemical and localization studies. Utilizing analytical chemistry-based approach, it was observed that overexpressing lines of *Arabidopsis* showed changes in the composition of cell-wall polysaccharides especially in the levels of AG, AX and cellulose. These evidences suggested that plant VIH2 is an important component for cell-wall reinforcement to provide the overall mechanical support.

Until recently, two VIH (initially referred as VIP) genes have been identified in model plant *Arabidopsis* and subsequent characterization showed their role in plant defense by modulating the jasmonate-dependent pathway[16,17]. Recently studies investigating inositol pyrophosphates have gained much attention[4,9,29]. We identified two *Vip*-like homologs (*VIH* genes) from wheat genome, which were studied for their evolutionary relationships and detailed expression characterization. This study was planned to identify the functional role of plant genes encoding for biosynthesis of PP-InsPx. Hexaploid bread wheat has one of the most complex genomes comprising of three related sub-genomes that have originated from three separate diploid ancestors thus forming an allohexaploid genome[30,31]. Therefore, to consider the appropriate homoeolog-transcript for further studies, Wheat-Exp expression database was used for checking VIH2 expression in different tissues and also during developmental time course (Figure S2). VIH2 is known to be involved in defence response via a jasmonate-dependent resistance in *Arabidopsis*[17]. We find late expression (72 hrs post infection) of VIH genes upon infection with Stripe rust and powdery mildew (Figure S2). Thus, the role of plant VIH genes during plant-microbe interaction was found to be conserved.

We demonstrated that TaVIH kinase domain has the ability to catalyse the phosphorylation of $InsP_6$ to form pyrophosphate species using ADP-GLO max assay (Figure 3C). This bioluminescence-based kinase assay has been demonstrated and validated as a high throughput assay overcoming the challenges imposed by high ATP concentrations[32]. Hence, our kinase assays revealed that wheat VIH proteins show $InsP_6$ kinase/Vip1like activity. Similarly, yeast and human enzymes also demonstrated $InsP_6$ and $InsP_7$ kinase activity[15,33,34]. Our TaVIH2-3B showed highest homology to AtVIH2 (70.6 %). In past, *AtVIH* genes have been shown to be biochemically active for kinase activity that generates $InsP_7$ and $InsP_8$[16,17]. Our study lacked these biochemical evidences, yet complementation activity and homology of wheat VIH2-3B to AtVIH2, indicates that it should also act in similar manner as AtVIH2. Additionally, we exploited the sensitivity of *vip1Δ* strain towards 6-Azauracil to validate the function of *TaVIH* genes. Our growth assay experiments with two different

404 concentrations of 6-azauracil substantiate that wheat homoeologous VIH2-3B was resistant
405 to 6-Azauracil as in case of AtVIH2 (Figure 3D)[17,22].

406 The presence of various *cis*-acting elements in the promoter regions play essential
407 roles in transcriptional regulation of genes in response to multiple environmental factors.
408 The transcriptional activity of *TaVIH2* promoter and differential expression analysis link
409 TaVIH2 with Pi-starvation response (Figure S4, Figure 4). This function of inositol
410 pyrophosphate kinases in the regulation of Pi homeostasis seems to be evolutionarily
411 conserved[4,34]. In general, various form of inositol phosphates reported previously have been
412 involved during low Pi responses[34,35]. Moreover, *IPK1* mutants of *Arabidospsis* showed
413 enhanced sensitivity for Pi and also have increased mobilization of Pi from roots to
414 shoots[36,37]. Very recently in *Arabidopsis*, it was demonstrated that VIH derived $InsP_8$ is
415 required to sense the cellular Pi status and also binds to the intracellular Pi sensor SPX1 to
416 control Pi homeostasis in plants[38]. Additional evidences also point towards that plant VIH
417 could modulation of cellular ATP concentration and thereby effects the PPInsP levels to
418 maintain the cellular Pi and its starvation responses[39]. Our *VIH2promoter:GUS* expression
419 under Pi-limiting stress and other accumulating evidences point the upcoming function for
420 VIH derived inositol pyrophosphate such as $InsP_8$ in Pi-homeostasis. Bound form of Pi in
421 plants referred to as $InsP_6$ accumulates in seeds of cereal crops as stored P, that is utilised
422 during the seed germination and development[40]. Multiple reports have linked *lpa* (low
423 $InsP_6$) mutations with alterations in accumulation of inositol pyrophosphates[16,41]. *Atmrp5*
424 mutants with reduced amount of $InsP_6$ and higher levels of Pi tend to accumulate more
425 amount of $InsP_7$ and $InsP_8$[16]. The higher expression of *VIH* genes in low $InsP_6$ wheat RNAi
426 lines targeting *TaABCC13* or *TaIPK1* also support these observations (Supplementary
427 Figure S8). Similarly, expression analysis of *lpa-Glycine max* also resulted in 1.9 fold
428 upregulation in seed-specific expression of *GLYMA_18G255000* that is an orthologue of
429 *VIH* genes[42]. The changes in expression of *TaVIH* genes in low $InsP_6$ lines suggests
430 correlation between $InsP_6$ biosynthesis and altered accumulation of $InsP_7$ and $InsP_8$. However,
431 a direct contribution of *VIH* genes in regulation of phosphate homeostasis is lacking and
432 needs detailed attention. These evidences suggest that, VIH proteins function in Pi
433 homeostasis like IPK1 (inositol penta*kis*phosphate kinase) and ITPKs (inositol tetraphosphate
434 kinase) although at different level[41]. Our expression studies showed that wheat *VIH* levels
435 were increased under drought condition. These observations are supported by the previous
436 study wherein, the changes in cellular levels of $InsP_7$ and $InsP_8$ have been attributed to guard
437 cell signalling and resistance to drought in maize *mrp5* mutants[4,43]. Altogether, the RNA-seq

profiling and qPCR-based expression studies of *TaVIH* genes showed induction of *TaVIH2* transcript under drought stress.

Y2H study led to the identification of TaFLA6 and multiple cell-wall reinforcement proteins as potential interactors of plant VIH proteins. Previously, it was shown that FLA proteins were involved in cell-wall reinforcement, plasticity, cell to cell adhesion and drought tolerance [44-48]. Cereal grains such as wheat are also rich in arabinogalactans such as FLA, associated with the yield of flour in the milling[49]. Expression of wheat *VIH* genes are highly abundant during late stage of grain maturation. Our qRT-PCR specifically indicates that both; wheat *VIH* and *FLA6* are co-expressed under drought condition, suggesting that they are involved in the similar pathway (Figure 7A). A strong *TaVIH2promoter:GUS* expression during dehydration indicates enhancedtranscriptional response during stress.

Previously, multiple *Arabidopsis* FLAs were reported to be perturbed under drought condition[50,51]. Recently, FLA-like protein was shown to be involved during the molecular responses of Pi deficiency that is mediated by the induced root hair elongation[52]. The domain analysis of FLA6 suggests it belonged to the category-IV of FLAs and show presence of all the necessary domains (FLA, AGP and GPI anchor) that is typical of this gene family (Figure 6D). Our Co-localization data for FLA6 and VIH2 in yeast points their interaction in the cytoplasmic region near the membrane. Overall, our data supports the role of plant VIH proteins during dehydration that could be concerted by FLA proteins in wheat. It is important to notice that additional VIH2 interacting clones encodes for glycosyltransferases, xylan-arabinosyl transferase and glycine-rich cell-wall structural like-protein. Surprisingly, genes encoding for glycosyltransferases, xylan-arabinosyl transferases are homoeologs (*TaGT* and *TaXat*) and belong to the family of transferases. The glycosyl and xylan arabinosyl transferases proteins are involved in the biosynthesis of polysaccharides for cell-wall biosynthesis[53,54]. Similarly, glycine-rich cell-wall proteins are recognized for their role in cell-wall reinforcement by callose deposition[55]. The high number of reoccurring clones related to cell-wall biosynthesis suggest important role that VIH proteins may offer during developmental stages. To confirm this, we constitutively expressed functionally active and dehydration responsive TaVIH2-3B protein in *Arabidopsis*. The VIH2-3B overexpression lines show robust growth and enhanced branching. The GC-MS profiling of TaVIH2-3B overexpressing lines showed increased accumulation of AG, AX and cellulose (Figure 9). These components are important for providing the overall mechanical strength to the plant cell and thereby tolerance to stress condition. Ratio of AG/AX are the representation of the quality of any given extraction procedure. Our extraction procedures for control plants show

the ratio of 1::1.2 to 1.5 for arabinose/galactose and arabinose/xylans. This ratio was perturbed in TaVIH2 overexpressing lines and *Atvih2-3* mutant lines. Previously it was suggested that *Atvih2-3* lacked mRNA expression of *VIH2* and have also have low levels of $InsP_8$[17]. The *VIH2* mutant in *Arabidopsis* are more susceptible to infestation by caterpillar (*Pieris rapae*) and thrips [17]. Additionally, it was suggested that resistance against herbivore pathogens such as *P. rapae*, could be gained by modulating the genes associated with cell-wall modification[56]. *Arabidopsis VIH2* mutant lines showed compositional changes in the cell-wall extracted polysaccharides especially in the AG levels (Figure 9). Therefore, the decreased resistance in VIH2 mutants against herbivores could be accounted for the defect in signalling pathway via COI1-dependent gene regulation and the contribution due to changes in the structural composition of the cell-wall. Earlier, it was also proven that inositol polyphosphate kinase activity of Kcs1p was required for adaptive changes in the yeast cell-wall under stress condition[57]. Protein-protein interaction-based studies are important to provide associated functional clues. Earlier, it was shown that yeast Vip1p interacts with histone H3/H4 chaperone, Asf1p. Vip1p and Asp1p counterparts in *S. pombe* functionally regulate actin-related protein-2/3 complexes and thereby participate in the fate of cell morphology[22]. Plant Kcs1 is still not known, yet it seems that as in case of yeast plant VIH may influence cell-wall properties. Taken together it may be inferred that VIH2 protein can causes changes in the plant cell-wall composition especially in the levels of important polysaccharides. In summary, our work along with the previous functional reports suggested an emerging novel roles of plant VIH proteins in cell-wall maintenance and/or reinforcement to provide resistance against dehydration or drought stress.

Methods

Plant materials and growth conditions

The experimentation in this study was conducted using Bread wheat (*Triticum aestivum* L.) variety C306, a rain-fed cultivar which is well known for its better processing quality. For collection of the tissue materials, the spikes were tagged at the first day after anthesis (DAA). Samples were collected in the form of spikes at 7, 14, 21 and 28 DAA stages and various tissues, including root, stem, leaf and flag leaf at 14 DAA stage respectively. To further dissect the expression levels in spikelet's, 14 DAA seed was used to separate different tissues, including aleurone, endosperm, embryo, glumes and rachis as done previously[24].

In order to perform stress related experiments, wheat seeds were surface sterilized using 1.2% Sodium Hypochlorite solution in 10% ethanol for 5-7 mins with continuous shaking followed by four washes with autoclaved MQ. The sterilized seeds were allowed to germinate on Whatman filter paper soaked in water for 3-5 days. The germinated seedlings with their residual endosperm excised, were transferred to Hoagland's nutrient media in phytaboxes with 10 seedlings in each box. For phosphate starvation experiment, 7-day old seedlings were subjected to Pi-sufficient nutrient condition by supplementing them with 200 µM KH_2PO_4 and Pi-deficient nutrient condition using 10 µM KH_2PO_4. The root and shoot samples were harvested at four different stages: 5, 10, 15 and 20 days of starvation[24]. For drought stress experiment, the seedlings were allowed to grow in Hoagland's media containing 5% PEG-8000[58] and samples collected 72 hrs after stress treatment. The hydroponic culture was carried out in a growth chamber set at 22 ± 1 °C, 50–70 % relative humidity and a photon rate of 300 µmol photons m^{-2} s^{-1} with a 16 h light/8 h dark cycle.

Isolation of total RNA, cDNA synthesis and quantitative real time PCR analysis

The harvested tissue samples were snap frozen in liquid nitrogen and stored at -80˚C for subsequent RNA isolation. Total RNA from various tissues was extracted by manual method using TRIzol® Reagent (Invitrogen™). The integrity of RNA and concentration was measured using NanoDrop™ Lite Spectrophotometer (Thermo Fisher Scientific, United States). The contamination of genomic DNA was removed by subjecting the RNA samples to DNase treatment using TURBO™ DNase (Ambion, Life Technologies). 2µg of total RNA was used for cDNA preparation using The Invitrogen SuperScript III First-Strand Synthesis System SuperMix (Thermo Fisher Scientific) as per the manufacturer's guidelines.

In order to quantify the gene expression, qRT-PCR was performed using the QuantiTect SYBR Green RT-PCR Kit (Qiagen, Germany). The gene specific primers capable of amplifying 150-250 bp region from all the three homoeologous of both *TaVIH* genes were carefully designed using Oligocalc software. Four technical replicates for each set of primers and minimum of 2 experimental replicates were used to validate the experiment. Gene specific primer used in the study are listed in Table S4. ADP-ribosylation factor gene (*TaARF*) was used as an internal control in all the expression studies. The Ct values obtained after the run were normalized against the internal control and relative expression was quantified using $2^{-\Delta\Delta C_T}$ method[59]. For In-silico expression for *TaVIH* genes in different tissues and stresses, wheat VIH RefSeq IDs were used to extract expression values as TPMs

from expVIP database. For different tissues and stages, the expression values were used to build a heatmap. In case of abiotic and biotic stress conditions, the expression values from the control and stressed conditions were used to get fold change values, which were then used to plot heatmaps using MeV software.

Identification and cloning of two wheat *VIH* genes

Two *Arabidopsis* (AT5G15070.2 and AT3G01310.2) and the previously reported yeast VIP1 sequences were used to perform Blastx analysis against the IWGSC (www.wheatgenome.org/) and wheat EST databases. The identified EST sequences were checked for the presence of the typical dual domain structure. Further, screening of these sequences resulted in the identification of two different genomic locations (Table S1). Furthermore, the Pfam domain identifiers of the signature ATP-Grasp Kinase (PF08443) and Histidine Acid Phosphatase (PF00328) domains were used to identify VIP proteins in Ensembl database using BioMart application. The corresponding predicted homoelogous transcripts were identified and compared to the other VIH sequences. DNA STAR Lasergene 11 Core Suite was used to perform the multiple sequence alignment and to calculate the sequence similarity. Gene specific primers capable of amplifying the transcript from the specific genome was designed after performing 5` and 3`-RACE to ascertain the completed open reading frame (ORF). Subsequently, full length primers were designed to amplify the *VIH* genes. The generated full-length sequence information was further used for qRT-PCR related studies.

Homology modelling and hydropathy plot

Homology modelling was performed for VIH1-4D & VIH2-3B based on their ATP-grasp domains (residues 7 to 332 for VIH1-4D and 12 to 339 for VIH2-3B), which share an identity of ~57% with hPPIP5K2 (residues 41 to 366). In both cases, the align2d command in MODELLER[60] was used to align TaVIHs against hPPIP5K2 and the 3D models with ANP, IHP and 4 Mg^{2+} ions fitted in were calculated using the automodel class. Best models were selected based on the MODELLER objective function. The models were visualized using UCSF Chimera[61]. The hydropathy profile for proteins was calculated according to Kyte and Doolittle., 1982. The positive values indicate hydrophobic domains and negative values represent hydrophilic regions of the amino acid residues.

In-vitro translation of TaVIH proteins and kinase assay

In order to study the kinase activity of TaVIHs, the proteins for kinase domains were synthesized using PURExpress *In-Vitro* Protein Synthesis Kit (NEB). The kinase assays were performed using the ADP-Glo™ Max Assay kit (Promega) as described earlier (Wormald et al., 2017). The kinase domains of *TaVIHs* [1-328aa for TaVIH1(4D) and 1-345aa for TaVIH2(3B)] cloned into pET23a vector system were used as template for setting up the reaction for protein synthesis as per manufacturer's protocol. The desired protein bands were further confirmed by running a western using HRP-conjugated T7 antibody against the T7 tag present at the N-terminal of the recombinant protein. The kinase assays were performed using the ADP-Glo™ Max Assay kit (Promega) as per the manufacturer's protocol. Two different substrate concentrations (40 and 80 µM) of $InsP_6$ (Calbiochem, Germany) were used. The recorded luminescence gives the measure of ADP produced in the kinase reaction and hence is proportional to the kinase activity.

Cloning of VIH promoters, analysis for cis-element and construction of GUS fused reporter

The sequence information of promoter regions of *TaVIH* genes was retrieved from Ensembl database as mentioned earlier. About 1600-1800 bp fragments upstream of the start codon were PCR amplified. From Genomic DNA of cv. C306 and cloned into pJET1.2 (Clonetech) cloning vector. The cloned DNA fragments were sequenced confirmed and inserted into pCAMBIA1391z, a promoter-less binary vector containing GUS reporter gene, using forward and reverse primers with Bam*HI* and Nco*I* sites respectively to form a *TaVIHpromoter:GUS* fusion construct. The promoter sequences of *TaVIH* genes were analysed for the presence of cis-regulatory elements using PLANTCARE database (http://bioinformatics.psb.ugent.be/webtools/plantcare/). Apart from this, various cis-elements involved in regulation of multiple abiotic and biotic stress conditions were curated manually through literature survey. The *VIHPromoter:GUS* fusion constructs were transformed into *Agrobacterium tumefaciens* GV3101 strain and introduced into *Arabidopsis* plants using *Agrobacterium* mediated transformation by floral dip method[62]. Three to four weeks old plants grown at 22 ± 1 °C, 16 h light/8 h dark cycle and a photon rate of 100 µmol photons m^{-2} s^{-1} were used for transformation. The independent transformants were screened on 0.5X MS media containing 30 mg/L hygromycin and 0.8% agar. The transformed seedlings with long hypocotyls and green expanded leaves at 4-leaf stage were separated out from the non-transformed seedlings and transferred to soil after about 3

607 weeks[63]. In a similar manner T_1 and T_2 generation seeds were also selected and allowed to
608 grow till maturity. The transgenics were confirmed for the presence of recombinant cassette
609 using PCR based approach. The transgenic lines harbouring empty pCAMBIA1391z vector
610 was used as a negative control. The PCR positive lines were further used for functional
611 characterization of promoter.

612

613 **Abiotic stress treatments to VIHpromoter:GUS transgenic seedlings and histochemical**
614 **GUS assay**

615 For promoter analysis, the seeds of PCR positive lines were surface sterilized and grown on
616 0.5X MS (Murashige and Skoog media) agar plates containing 30 mg/L Hygromycin B for
617 15 days before they were subjected to various abiotic stress and hormonal treatments[64]. For
618 dehydration stress, the seedlings were air dried by placing them on Whatman filter paper for
619 1hr. Heat treatment was given by incubating the seedlings at 37˚C for 8hrs. Hormonal
620 treatment including ABA (100 µM), GA_3 (20 µM) and abiotic stress including salt (300 mM)
621 and drought (20% PEG) were given by placing the seedlings on filter paper impregnated with
622 0.5X MS solution containing the respective chemical. The treatment continued for 24 hrs
623 before subjecting them to histochemical staining. For subjecting the seedlings to low
624 phosphate stress conditions, they were allowed to grow on 0.5X MS agar plates without
625 KH_2PO_4 for 96 hrs. The seedlings placed on filter paper dipped with MS solution without any
626 chemical served as a control and histochemical GUS staining carried out[65]. Two weeks old
627 seedlings after respective treatments were incubated overnight in GUS staining solution
628 containing 50 mM sodium phosphate buffer (pH 7.2), 2 mM potassium ferricyanide, 2 mM
629 potassium ferrocyanide, 20% (v/v) methanol, 0.2% (v/v) Triton-X100 and 2 mM X-Gluc
630 (HiMedia, India) at 37 ˚C in a 48-well microplate containing about 10 seedlings/well.
631 Chlorophyll was removed from tissues by dipping in 90% ethanol. The staining was
632 visualized and photographed under Leica DFC295 stereomicroscope (Wetzlar, Germany) at
633 magnification of 6.3X

634

635 **Construct preparation for expression vector and yeast functional complementation**

636 For complementation assays, pYES2, a galactose-inducible yeast expression vector was used.
637 The functional complementation of yeast by TaVIH proteins was studied using 6-azauracil
638 based assay [17,24]. The wild type BY4741 (MATa; his3D1; leu2D0; met15D0; ura3D0) and
639 *vip1Δ* (BY4741; MATa; ura3Δ0; leu2Δ0; his3Δ1; met15Δ0; YLR410w::kanMX4) yeast strains

were used for the growth assays. The CDS corresponding to the catalytic domain of *ScVIP1* (1-535 amino acids) cloned into pYES2 expression vector was used as a positive control. *TaVIH1/2* along with *ScVIP1* and empty vector were transformed individually into wild type and mutant strains by lithium acetate method with slight modifications. For growth assay, the wild type and mutant *S. cerevisiae* strains carrying different plasmids were allowed to grow overnight in minimal media without uracil. The primary culture was used to re-inoculate fresh media to an OD_{600} of 0.1 and allowed to grow till the culture attained an optical density of 0.6-0.8. The cell cultures were then adjusted to O.D of 1 and further serially diluted to the final concentrations of 1:10, 1:100 and 1:1000. 10 µl each of these cell suspensions were used for spotting on SD(-Ura) plates containing 2% galactose, 1% raffinose and varying concentrations of 6-azauracil (0, 2.5 and 5 mM). The colony plates were incubated at 30ºC and pictures were taken after 4 days.

Wheat cDNA Library construction, yeast two-hybrid screening and pull-down assays

The total RNA (~120 µg) samples were pooled from the vegetative tissues including shoots and roots. From the isolated total RNA, mRNA purification was performed by using (NucleoTrap mRNA mini kit, Macherey-Nagel, Germany). A total of 0.25 µg mRNA was used to make the cDNA library (Make & Plate^{TM} Library System, Clontech, USA). The wheat cDNA library was prepared and purified using CHROMA SPIN+TE-400 columns. A cDNA fragment sizes of <2kb was used for the library screening using TaVIH2 as a bait. The library shows the titre value of ~$0.8x10^9$ cfu/ml. Yeast two-hybrid assays and screening were performed by using GAL4-based screening system (Matchmaker Gold Yeast Two-hybrid System, Takara Inc., USA). Most of the steps were followed as per manufacturer's instructions unless mentioned. Briefly, putative positive interacting clones were obtained when the competent yeast strain Y187 was co-transformed with cDNAlibrary+AD (pGADT7-Rec vector) and Y2H-Gold containing BD vector (*TaVIH2-3B:pGBKT7* bait vector) respectively. Following stringent screening procedures, putative clones were obtained and screened for their reporter assays (along with Aureobasidin A). Full length ORF was cloned for the gene of interest and one-on-one interaction was also done to confirm its interaction. Routine yeast transformation was done by using Yeastmaker Yeast transformation System 2 (Clontech, USA).

For pull down assays respective yeast cultures were grown in SD media with appropriate amino acid dropouts. The primary culture was grown for overnight at 30 ˚C until a OD_{600} of 1 was achieved. The secondary culture was incubated for 6 hrs and cells were

washed and lysate was prepared by using glass bead in buffer (1% SDS, 100mM NaCl,100mM Tris-Cl, 1mM EDTA, 2% Triton and 1mM protease inhibitor (100X Halt protease inhibitor, Thermofisher, USA). The protein concentration in lysate was calculated at two dilutions. Equal amount of each lysate was taken and incubated with 100% of Protein-G agarose beads as well as 2 ul of anti-c-Myc antibody for overnight at 4 ˚C. The lysate was subsequently washed for three times with lysis buffer and centrifuged for 30 sec at 800 x g. 50 ul of loading dye was added to the washed beads and heated at 65 C for 10 min. After SDS-PAGE run the proteins was transfer to PVDF membrane and was processed. Blot was separated into two p arts to detect TaVIH2 and TaFLA6 separately. Different primary antibodies were used for probing (mouse Anti-c-myc and rabbit anti-HA with 1:2000 dilution). After washing the blots with TBST, they were treated with the secondary antibody (Goat Anti-Mouse IgG (H + L); and Goat Anti-Rabbit IgG (H + L) with 1:5000 dilution. After subsequent washing with TBST the blot was developed by using BIO-RAD clarity western ECL Substrate.

Protein localization

For the localization experiments *TaFLA6* was cloned in pGADT7 vector at *Eco*R1 and *Bam*H1 sites. *TaVIH2* cDNA was cloned in pGBKT7 vector using *Sma*1 and *Not*1 restriction sites. The constructs were transformed in Y2H Gold yeast strain and selected on SD-Leu or SD-Trp plates respectively. Yeast spheroplasts were prepared for localization as described earlier (Severance et al., 2004). Mouse monoclonal Anti-HA (HA:FLA6-pGADT7): or rabbit Anti-c-Myc (cMYC:VIH2-pGBKT7) primary antibody (Invitrogen, USA) was used for the respective preparations, at a ratio of 1:200 followed by 5 washing with blocking buffer. Yeast cells were incubated with Goat Anti- Mouse IgG (H+L) Alexa Flour Plus 488 or Goat Anti-Rabbit IgG (H+L) Alexa Flour Plus 647 (Invitrogen, USA) at a ratio of 1:500 for 4hr at room temperature. Cells were washed with blocking buffer and mounted with Fluor mount (Sigma, USA). Representative fluorescent images were taken using Zeiss fluorescence microscope Axio Imager Z2 with an Axiocam MRm camera at 63X of magnification.

Measurement of relative water content

Relative water content (RWC) was performed as mentioned earlier[66]. The value for each treatment were calculated by using the standard formula RWC (%) = [(FW-DW)/(TW-DW)] X 100[67] with FW is fresh weight, DW is dry weight and TW is turgor weight. For performing the experiments, leaves of equal sizes were detached from transgenic lines and control

Arabidopsis undergoing dehydration (at 12, 19 and 24 days) were collected and weighed immediately (FW). The leaves were submerged in deionized water for 24 hrs. After incubation the leaves were blotted dry and their weight was determined (TW). To measure their DW, they were oven dried (at 65 ^{o}C) for 24 hrs. The experiments were performed with at least three experimental replicates each consisting of five to six plants.

Extraction and GC-MS analysis of *Arabidopsis* cell-wall polysaccharides

Extraction of cell-wall components was performed as described earlier[68]. Briefly, five grams (fresh weight) of shoots from respective lines (~25 days old) was crushed to a fine powder in liquid nitrogen. The power of the tissue was treated with 3% Na_2CO_3 at 4 °C for 8 hrs followed by centrifugation. Pellet was further used separately for extraction of Arabinoxylan (AX) and Cellulose. The remaining supernatant was processed for extracting arabinogalactan (AG) by neutralizing with glacial acetic acid and performing dialysis (20 L * 6 times) for three days. Post dialysis samples were concentrated with rotary evaporator and then lyophilized to measure AG. The pellet was treated with 5 M NaOH solution containing 5 mg of $NaBH_4$ at 80°C for 2hr. The alkali extracted material was centrifuged. Pellet was washed with deionized water 2-3 times and dried to obtain cellulose. Remaining supernatant was neutralized with glacial acetic acid for AX. The respective neutralized extracts were dialyzed, concentrated and precipitated with ethanol (3 vol.) and centrifuged. Precipitated residue was finally lyophilized to prepare AX.

For compositional analysis the extracted AG, AX and Cellulose were determined by preparing their alditol derivatives. Extracted AG and AX were separately hydrolysed with 2M trifluoroacetic acid at 110 °C for 2.5 hr. Hydrolysis of cellulose was done in two steps that includes primary hydrolysis in 72 % H_2SO_4 at 30 °C for 1 hr followed by sample dilution upto 4 % H_2SO_4 concentration and again subjected to secondary hydrolysis at 121 °C for 1 hr. The solution was neutralized with $BaCO_3$ and further reduction was done with $NaBH_4$ (20 mg) followed by acetylated with mixture of acetic anhydride and pyridine (1:1) at 100°C for 1 hr to prepare alditol acetate derivatives. Derivatized monosaccharides were analysed with GC instrument coupled to a mass spectrometer. 2ul sample was introduced in the split less injection mode in DB-5 (60 m × 0.25 mm, 1 µm film thickness, Agilent, CA) using helium as a carrier gas. The alditiol acetate derivative were separated using the following temperature gradient: 80 °C for 2 min, 80-170 °C at 30°C/min, 170-240 °C at 4°C/min, 240 °C held for 30 min and the samples were ionized by electrons impact at 70 eV.

742 **Author contributions**

743 Conceptualization: MK, AS and AKP; Methodology: AKP, MK, AS, KB, KM, SK and SS;
744 Investigation: MK, AS, SS, SA, AK, AKP, PP and VR; Writing-Original Draft: AKP, MK,
745 and PP; Writing Review & Editing: AKP, VS, VR, KM, KB and PP; Funding Acquisition:
746 AKP and VR; Resources: SA, KB, SK and GK; Supervision, AKP, VR and PP.
747

748 **Acknowledgement**

749 Authors thank Executive Director for facilities and support. This study was supported by
750 Department of Biotechnology, Basic Plant Biology Grant to AKP and VR
751 [BT/PR12432/BPA/118/35/2014]. Part of this work was also supported by NABI-CORE grant
752 to AKP. Yeast strain *vip1Δ* and ScVIP1 was kindly gifted by Dr. Rashna Bhandari (CDFD).
753 MK thank UGC-CSIR for her research scholarship. Thanks to Dr. Gabriel Schaff for sharing
754 the *Arabidopsis vih2-3* mutant. AS thank DBT for SRF fellowship. DBT-eLibrary Consortium
755 (DeLCON) is acknowledged for providing timely support and access to e-resources for this
756 work.
757

758 **Data availability**

759 The resources including plasmids, constructs and transgenic *Arabidopsis* seeds will be available
760 upon request.
761

762 **References:**

763 1. Hegeman, C. E., Good, L. L. & Grabau, E. A. Expression of d- *myo* -Inositol-3-
764 Phosphate Synthase in Soybean. Implications for Phytic Acid Biosynthesis. *Plant*
765 *Physiol.* **125**, 1941–1948 (2001).
766 2. Shears, S. B. Intimate connections: Inositol pyrophosphates at the interface of
767 metabolic regulation and cell signaling. *J. Cell. Physiol.* **233**, 1897–1912 (2018).
768 3. Stephens, L. *et al.* The detection, purification, structural characterization, and
769 metabolism of diphosphoinositol pentakisphosphate(s) and bisdiphosphoinositol
770 tetrakisphosphate(s). *J. Biol. Chem.* **268**, 4009–15 (1993).
771 4. Williams, S. P., Gillaspy, G. E. & Perera, I. Y. Biosynthesis and possible functions of
772 inositol pyrophosphates in plants. *Front. Plant Sci.* **6**, 67 (2015).
773 5. Bennett, M., Onnebo, S. M. N., Azevedo, C. & Saiardi, A. Inositol pyrophosphates:
774 metabolism and signaling. *Cell. Mol. Life Sci.* **63**, 552–564 (2006).

6. York, S. J., Armbruster, B. N., Greenwell, P., Petes, T. D. & York, J. D. Inositol Diphosphate Signaling Regulates Telomere Length. *J. Biol. Chem.* **280**, 4264–4269 (2005).
7. Luo, H. R. *et al.* Inositol pyrophosphates are required for DNA hyperrecombination in protein kinase c1 mutant yeast. *Biochemistry* **41**, 2509–15 (2002).
8. Saiardi, A. How inositol pyrophosphates control cellular phosphate homeostasis? *Adv. Biol. Regul.* **52**, 351–359 (2012).
9. Jadav, R. S., Chanduri, M. V. L., Sengupta, S. & Bhandari, R. Inositol Pyrophosphate Synthesis by Inositol Hexakisphosphate Kinase 1 Is Required for Homologous Recombination Repair. *J. Biol. Chem.* **288**, 3312–3321 (2013).
10. Voglmaier, S. M. *et al.* Purified inositol hexakisphosphate kinase is an ATP synthase: diphosphoinositol pentakisphosphate as a high-energy phosphate donor. *Proc. Natl. Acad. Sci.* **93**, 4305–4310 (1996).
11. Saiardi, A., Erdjument-Bromage, H., Snowman, A. M., Tempst, P. & Snyder, S. H. Synthesis of diphosphoinositol pentakisphosphate by a newly identified family of higher inositol polyphosphate kinases. *Curr. Biol.* **9**, 1323–6 (1999).
12. Draškovič, P. *et al.* Inositol Hexakisphosphate Kinase Products Contain Diphosphate and Triphosphate Groups. *Chem. Biol.* **15**, 274–286 (2008).
13. Choi, J. H., Williams, J., Cho, J., Falck, J. R. & Shears, S. B. Purification, sequencing, and molecular identification of a mammalian PP-InsP5 kinase that is activated when cells are exposed to hyperosmotic stress. *J. Biol. Chem.* **282**, 30763–75 (2007).
14. Fridy, P. C., Otto, J. C., Dollins, D. E. & York, J. D. Cloning and Characterization of Two Human *VIP1* -like Inositol Hexakisphosphate and Diphosphoinositol Pentakisphosphate Kinases. *J. Biol. Chem.* **282**, 30754–30762 (2007).
15. Mulugu, S. *et al.* A Conserved Family of Enzymes That Phosphorylate Inositol Hexakisphosphate. *Science (80-.).* **316**, 106–109 (2007).
16. Desai, M. *et al.* Two inositol hexakisphosphate kinases drive inositol pyrophosphate synthesis in plants. *Plant J.* **80**, 642–653 (2014).
17. Laha, D. *et al.* VIH2 Regulates the Synthesis of Inositol Pyrophosphate InsP8 and Jasmonate-Dependent Defenses in Arabidopsis. *Plant Cell* **27**, 1082–97 (2015).
18. Wild, R. *et al.* Control of eukaryotic phosphate homeostasis by inositol polyphosphate sensor domains. *Science (80-.).* **352**, 986–990 (2016).
19. Kornberg, A., Rao, N. N. & Ault-Riché, D. Inorganic Polyphosphate: A Molecule of Many Functions. *Annu. Rev. Biochem.* **68**, 89–125 (1999).

20. Rao, N. N., Gómez-García, M. R. & Kornberg, A. Inorganic Polyphosphate: Essential for Growth and Survival. *Annu. Rev. Biochem.* **78**, 605–647 (2009).
21. Azevedo, C. & Saiardi, A. Eukaryotic Phosphate Homeostasis: The Inositol Pyrophosphate Perspective. *Trends Biochem. Sci.* **42**, 219–231 (2017).
22. Osada, S. *et al.* Inositol phosphate kinase Vip1p interacts with histone chaperone Asf1p in Saccharomyces cerevisiae. *Mol. Biol. Rep.* **39**, 4989–4996 (2012).
23. Dorsch, J. A. *et al.* Seed phosphorus and inositol phosphate phenotype of barley low phytic acid genotypes. *Phytochemistry* **62**, 691–706 (2003).
24. Shukla, V. *et al.* Tissue specific transcript profiling of wheat phosphate transporter genes and its association with phosphate allocation in grains. *Sci. Rep.* **6**, 39293 (2016).
25. Johnson, K. L., Jones, B. J., Bacic, A. & Schultz, C. J. The Fasciclin-Like Arabinogalactan Proteins of Arabidopsis. A Multigene Family of Putative Cell Adhesion Molecules 1. (2003). doi:10.1104/pp.103.031237
26. Schultz, C., Gilson, P., Oxley, D., Youl, J. & Bacic, A. GPI-anchors on arabinogalactan-proteins: implications for signalling in plants. *Trends Plant Sci.* **3**, 426–431 (1998).
27. Saha, S., Anilkumar, A. A. & Mayor, S. GPI-anchored protein organization and dynamics at the cell surface. *J. Lipid Res.* **57**, 159–175 (2016).
28. Gillmor, C. S. *et al.* Glycosylphosphatidylinositol-anchored proteins are required for cell wall synthesis and morphogenesis in Arabidopsis. *Plant Cell* **17**, 1128–40 (2005).
29. Chakraborty, A., Kim, S. & Snyder, S. H. Inositol pyrophosphates as mammalian cell signals. *Sci. Signal.* **4**, re1 (2011).
30. Huang, S. *et al.* Genes encoding plastid acetyl-CoA carboxylase and 3-phosphoglycerate kinase of the Triticum/Aegilops complex and the evolutionary history of polyploid wheat. *Proc. Natl. Acad. Sci.* **99**, 8133–8138 (2002).
31. Dvorak, J. & Akhunov, E. D. Tempos of gene locus deletions and duplications and their relationship to recombination rate during diploid and polyploid evolution in the Aegilops-Triticum alliance. *Genetics* **171**, 323–32 (2005).
32. Wormald, M., Liao, G., Kimos, M., Barrow, J. & Wei, H. Development of a homogenous high-throughput assay for inositol hexakisphosphate kinase 1 activity. *PLoS One* **12**, e0188852 (2017).

33. Choi, K., Mollapour, E. & Shears, S. B. Signal transduction during environmental stress: InsP8 operates within highly restricted contexts. *Cell. Signal.* **17**, 1533–1541 (2005).

34. Lee, Y.-S., Mulugu, S., York, J. D. & O'Shea, E. K. Regulation of a Cyclin-CDK-CDK Inhibitor Complex by Inositol Pyrophosphates. *Science (80-.).* **316**, 109–112 (2007).

35. Norbis, F. *et al.* Identification of a cDNA/protein leading to an increased Pi-uptake in Xenopus laevis oocytes. *J. Membr. Biol.* **156**, 19–24 (1997).

36. Stevenson-Paulik, J., Bastidas, R. J., Chiou, S.-T., Frye, R. A. & York, J. D. Generation of phytate-free seeds in Arabidopsis through disruption of inositol polyphosphate kinases. *Proc. Natl. Acad. Sci.* **102**, 12612–12617 (2005).

37. Kuo, H.-F. *et al.* Arabidopsis inositol pentakisphosphate 2-kinase, AtIPK1, is required for growth and modulates phosphate homeostasis at the transcriptional level. *Plant J.* **80**, 503–15 (2014).

38. Dong, J. *et al.* Inositol Pyrophosphate InsP8 Acts as an Intracellular Phosphate Signal in Arabidopsis. *Mol. Plant* (2019). doi:10.1016/J.MOLP.2019.08.002

39. Zhu, J. *et al.* Two bifunctional inositol pyrophosphate kinases/phosphatases control plant phosphate homeostasis. *bioRxiv* 467076 (2018). doi:10.1101/467076

40. Singh, S. P. *et al.* Pattern of iron distribution in maternal and filial tissues in wheat grains with contrasting levels of iron. *J. Exp. Bot.* **64**, 3249–60 (2013).

41. Kuo, H.-F. *et al.* Arabidopsis inositol phosphate kinases IPK1 and ITPK1 constitute a metabolic pathway in maintaining phosphate homeostasis. *Plant J.* **95**, 613–630 (2018).

42. Redekar, N. R. *et al.* Genome-wide transcriptome analyses of developing seeds from low and normal phytic acid soybean lines. *BMC Genomics* **16**, 1074 (2015).

43. Klein, M. *et al.* The plant multidrug resistance ABC transporter AtMRP5 is involved in guard cell hormonal signalling and water use. *Plant J.* **33**, 119–29 (2003).

44. Shi, H., Kim, Y., Guo, Y., Stevenson, B. & Zhu, J.-K. The Arabidopsis SOS5 locus encodes a putative cell surface adhesion protein and is required for normal cell expansion. *Plant Cell* **15**, 19–32 (2003).

45. Majewska-Sawka, A. & Nothnagel, E. A. The Multiple Roles of Arabinogalactan Proteins in Plant Development. *Plant Physiol.* **122**, 3–10 (2000).

873 46. MacMillan, C. P., Mansfield, S. D., Stachurski, Z. H., Evans, R. & Southerton, S. G.
874 Fasciclin-like arabinogalactan proteins: specialization for stem biomechanics and cell
875 wall architecture in Arabidopsis and Eucalyptus. *Plant J.* **62**, 689–703 (2010).
876 47. Huang, G.-Q. *et al.* Characterization of 19 novel cotton FLA genes and their
877 expression profiling in fiber development and in response to phytohormones and salt
878 stress. *Physiol. Plant.* **134**, 348–59 (2008).
879 48. Zang, L., Zheng, T. & Su, X. *Advances in research of fasciclin-like arabinogalactan*
880 *proteins (FLAs) in plants*. *POJ* **8**, (2015).
881 49. Nirmal, R. C., Furtado, A., Rangan, P. & Henry, R. J. Fasciclin-like arabinogalactan
882 protein gene expression is associated with yield of flour in the milling of wheat. *Sci.*
883 *Rep.* **7**, 12539 (2017).
884 50. No, E.-G. & Loopstra, C. A. Hormonal and developmental regulation of two
885 arabinogalactan-proteins in xylem of loblolly pine (Pinus taeda). *Physiol. Plant.* **110**,
886 524–529 (2000).
887 51. Cagnola, J. I. *et al.* Reduced expression of selected FASCICLIN-LIKE
888 ARABINOGALACTAN PROTEIN genes associates with the abortion of kernels in
889 field crops of Zea mays (maize) and of Arabidopsis seeds. *Plant. Cell Environ.* **41**,
890 661–674 (2018).
891 52. Kirchner, T. W. *et al.* Molecular Background of Pi Deficiency-Induced Root Hair
892 Growth in Brassica carinata - A Fasciclin-Like Arabinogalactan Protein Is Involved.
893 *Front. Plant Sci.* **9**, 1372 (2018).
894 53. Scheible, W.-R. & Pauly, M. Glycosyltransferases and cell wall biosynthesis: novel
895 players and insights. *Curr. Opin. Plant Biol.* **7**, 285–95 (2004).
896 54. Whitehead, C. *et al.* A glycosyl transferase family 43 protein involved in xylan
897 biosynthesis is associated with straw digestibility in Brachypodium distachyon. *New*
898 *Phytol.* **218**, 974–985 (2018).
899 55. Ueki, S. & Citovsky, V. Identification of an interactor of cadmium ion-induced
900 glycine-rich protein involved in regulation of callose levels in plant vasculature. *Proc.*
901 *Natl. Acad. Sci. U. S. A.* **102**, 12089–94 (2005).
902 56. De Vos, M. *et al.* The *Arabidopsis thaliana* Transcription Factor AtMYB102
903 Functions in Defense Against The Insect Herbivore *Pieris rapae*. *Plant Signal. Behav.*
904 **1**, 305–311 (2006).

905 57. Dubois, E. *et al.* In Saccharomyces cerevisiae, the inositol polyphosphate kinase
906 activity of Kcs1p is required for resistance to salt stress, cell wall integrity, and
907 vacuolar morphogenesis. *J. Biol. Chem.* **277**, 23755–63 (2002).
908
909 58. Ji, H. *et al.* PEG-mediated osmotic stress induces premature differentiation of the root
910 apical meristem and outgrowth of lateral roots in wheat. *J. Exp. Bot.* **65**, 4863–72
911 (2014).
912 59. Livak, K. J. & Schmittgen, T. D. Analysis of relative gene expression data using real-
913 time quantitative PCR and the 2(-Delta Delta C(T)) Method. *Methods* **25**, 402–8
914 (2001).
915 60. Eswar, N. *et al.* Comparative Protein Structure Modeling Using Modeller. *Curr.*
916 *Protoc. Bioinforma.* **15**, 5.6.1-5.6.30 (2006).
917 61. Pettersen, E. F. *et al.* UCSF Chimera?A visualization system for exploratory research
918 and analysis. *J. Comput. Chem.* **25**, 1605–1612 (2004).
919 62. Zhang, X., Henriques, R., Lin, S.-S., Niu, Q.-W. & Chua, N.-H. Agrobacterium-
920 mediated transformation of Arabidopsis thaliana using the floral dip method. *Nat.*
921 *Protoc.* **1**, 641–6 (2006).
922 63. Harrison, S. J. *et al.* A rapid and robust method of identifying transformed
923 Arabidopsis thaliana seedlings following floral dip transformation. *Plant Methods* **2**,
924 19 (2006).
925 64. Wang, N. N., Shih, M.-C. & Li, N. The GUS reporter-aided analysis of the promoter
926 activities of Arabidopsis ACC synthase genes AtACS4, AtACS5, and AtACS7
927 induced by hormones and stresses. *J. Exp. Bot.* **56**, 909–20 (2005).
928 65. Jefferson, R. A. Assaying chimeric genes in plants: The GUS gene fusion system.
929 *Plant Mol. Biol. Report.* **5**, 387–405 (1987).
930 66. Ding, Y., Avramova, Z. & Fromm, M. The Arabidopsis trithorax-like factor ATX1
931 functions in dehydration stress responses via ABA-dependent and ABA-independent
932 pathways. *Plant J.* **66**, 735–744 (2011).
933 67. Hewlett, J. D. & Kramer, P. J. The measurement of water deficits in broadleaf plants.
934 *Protoplasma* **57**, 381–391 (1963).
935 68. Zablackis, E., Huang, J., Müller, B., Darvill, A. G. & Albersheim, P. Characterization
936 of the cell-wall polysaccharides of Arabidopsis thaliana leaves. *Plant Physiol.* **107**,
937 1129–38 (1995).
938

939

940

941 **Legends for the Figures:**

942 **Figure 1. Neighbourhood-Joining phylogenetic tree and Evolutionary conservation of**
943 **VIH proteins across species.** (A) Neighbourhood-Joining phylogenetic tree of VIP proteins.
944 The full-length amino acid sequences of VIH proteins from various taxonomic groups were
945 used for the construction of phylogeny using MEGA7.0. The numbers along the nodes
946 represent the percentage of bootstrap values from 1000 replications. Sequence included are
947 wheat VIH proteins along with multiple plant species, humans, *Dictyostelium*,
948 *Chlamydomonas* and yeast. across species (*Homo sapiens*, AAH57395; *M. musculus*,
949 NP_848910; *Drosophila melanogaster*, CG14616-PE; *S. cerevisiae*, NP_013514 and *S.*
950 *pombe*, SPCC1672.06c. (B) Schematic representation of domain architecture of TaVIHs
951 deduced from CDD database: light gray rectangles indicate ATP Grasp/RimK Kinase domain
952 and dark gray coloured heaxgons correspond to Histidine Phosphatase superfamily.(B) A
953 multiple sequence alignment of VIP1 homologs from *Triticum aestivum, Arabidopsis*
954 *thaliana, Homo sapiens and Saccharomyces cerevisae* performed using MEGA7.0. The
955 conserved catalytic aspartic acid residue conserved in VIH (VIP) proteins is indicated by a
956 red star shape. The phosphorylated serine residues conserved among plant VIH proteins as
957 predicted by MUsite have been highlighted in box. The arrows indicate signature motifs of
958 histidine acid phosphatases, RHXXR and HD. (C) Exon-intron arrangement of *TaVIH* genes.
959 The gene structures were predicted using GSDS online tool. Exons are displayed as red
960 hexagons, Introns as lines and the blue boxes show the upstream/downstream regions. The
961 intron phases are represented in numbers 0, 1 and 2.

962 **Figure 2. Gene expression analysis of wheat VIH transcript in different tissue and seed**
963 **development.** Quantification of transcript accumulation of wheat *VIH* genes : (A) *TaVIH1*
964 and (B) *TaVIH2* in different tissues of a wheat plant. The cDNA prepared from 2µg of DNA
965 free-RNA isolated from root, stem, leaf and flag leaf tissues of a 14 DAA plant as template.
966 (C) Quantitative expression analysis of *TaVIH* genes at different seed maturation stages (7,
967 14, 21 and 28 days after anthesis). (D) Quantification of transcript accumulation of wheat
968 *VIH* genes in different tissues of 14 DAA seed (aleurone, Al; endosperm, En; embryo, Em;
969 glumes, Gl and and rachis, Ra. For qRT-PCR, cDNA was prepared from 2µg of DNA-free
970 RNA isolated from respective tissues. *TaARF* was used as an internal control for

normalization of Ct values. Each bar represents the mean of 4 replicates along with standard deviation of the mean. (E) Microarray based expression profiles of *TaVIH* genes. The data was generated using GENEVESTIGATOR (https://www.genevestigator.com/gv/plant.jsp).

Figure 3. 3D structure for TaVIH proteins based on homology modelling, *in-vitro* kinase activity and yeast complementation assays. (A) TaVIH2-3B overall structure depicting the AMP-PNP ligand accommodated by two anti-paralled beta-sheets. (B) hPPIP5K2, TaVIH1-4D, and TaVIH2-3B depicting the conserved catalytic residues in the IP6/IHP binding pocket. The key conserved residues are depicted using sticks and the green spheres represent Mg^{2+} ions. (C) The relative luminescence units for all reactions performed were recorded using Spectramax optical reader. The kinase reactions were performed in 25µl:25µl:50µl ratio using ADP Glo max assay kit. The experiments were repeated 3 times using 3 different IVT reactions and similar response was obtained. (D**)** Yeast complementation assay for *TaVIH* genes. Representative image of spotting assay performed on SD-Ura plates containing 1% raffinose, 2% galactose and supplemented with 0, 2.5 and 5mM of 6-azauracil. The wild type BY4741 and *vip1Δ* strains were transformed with respective constructs using Li-acetate method. Representative images were taken 4 days after spotting assay was performed. Similar results were obtained with three independent repeats.

Figure 4. Analysis of VIH promoters for their cis-elements and their expression under different stress conditions. (A) Schematic representation of promoter regions of *TaVIH* genes. Putative cis regulatory elements responsible for hormonal as well as abiotic stress response present in 1000 bp region upstream of ATG have been indicated in different shapes. The positions of these motifs were deduced from sequence search by PLANTCARE database. (B) Hormonal and abiotic stress response of *TaVIH* genes promoter. Representative images for histochemical GUS assay performed against different stresses for promTaVIH1:GUS and promTaVIH2:GUS transgenic lines raised in Arabidopsis thaliana Col0 background. Two week old seedlings selected positive against hygromycin selection on 0.5XMS agar plates were subjected to respective treatments: 1hr air drying for dehydration, heat stress at 37 ˚C for 8hrs, (-)Pi condition: 0.5XMS medias without KH_2PO_4 for 96 hrs, ABA (100µM), GA_3 (20µM) and NaCl (300mM) and drought (20% PEG) for 24hrs. Seedlings with or without treatment (control) were stained overnight in GUS staining solution and photographed using Leica stereomicroscope at 6.3X magnification.

Figure 5. qRT-PCR analysis of the wheat VIH transcripts under different stress condition. (A) Relative quantification of *TaVIH* genes expression in Pi-limiting conditions.

The expression profiles of *TaVIH1* and *TaVIH2* in roots (Left panel) and shoots (Right panel) of wheat seedlings collected at 5, 10, 15 and 20 days of phosphate sufficient (P+) ie 200µM KH_2PO_4 and limiting (-P) conditions:10µM KH_2PO_4. qRT-PCR was performed as mentioned earlier. (B) Effect of PEG-8000 treatment on expression profiles of *TaVIH* genes. Relative quantification of *TaVIH1* and *TaVIH2* transcripts in Roots and Shoots of wheat seedlings after 72 hrs of treatment with 5% PEG-8000. cDNA templates were prepared from 2 µg RNA isolated from samples of CR-Control root, RT-Root treatment with PEG, CS-Control shoot and ST-Shoot treatment with PEG. The experiment included four replicates, the mean of which along with standard deviation was plotted to study the gene expression. The Ct values were normalized against the reference gene *TaARF*.

Figure 6. Interaction of TaVIH with TaFLA6 as identified during Y2H screening using TaVIH2-3B as a bait. (A) Y2H assay for the FLA6 and VIH interaction as represented by GAL plates containing -L-T and without GAL plates containing -HLT. (B) Pull down assay and Western analysis of the wheat FLA6 in the yeast strains. (C) Localization of FLA6 using HAtagged-TaFLA6 and TaVIH2 using cMYC tag. Fluorescence was measured using a Zeiss fluorescence microscope (Axio Imager Z2) with an Axiocam MRm camera at 63X. Representative images are shown and similar observations were noted for 3-4 independent transformed colonies of yeast. (D) Protein domain arrangement and hydrophobic plot for FLA6 domains with negative values represent hydrophilic regions.

Figure 7. Expression analysis of *TaFLA6, TaGT* and *TaXat.* (A) Differential expression of TaFLA6, TaGT/TaXat under drought condition in roots and shoots of wheat seedlings. (B) Relative gene expression level during grain development (7, 14, 21 and 28 DAA). (C) Gene expression profiles for the of the indicated genes using wheat expression database. For A and B, 2 µg RNA isolated from the given tissue and after cDNA synthesis gene specific primers were employed for expression studies. The Ct values were normalized against the reference gene *TaARF* as mentioned earlier.

Figure 8. Phenotypic analysis Arabidopsis transgenic lines and effect of water stress upon rehydration in leaves. (A) Western analysis of transgenic *Arabidopsis* lines overexpressing *TaVIH2-3B* -Line#2, Line#4, Line#5 and Line#6. (B) Phenotype of transgenic plants and length of the main shoot axis in mm. (C) Relative water content of Arabidopsis leaves during the drought treatment for period of 12, 19 and 24 days. Vertical bars represent the standard deviation. # on the bar indicates that the mean is significantly different at $p < 0.01$ with respect to their respective control treatments.

Figure 9. Polysaccharides composition of Arabidopsis shoots. For cell-wall composition analysis wildtype Col-O, *Arabidopsis* overexpressing TaVIH2-3B (Line#3 and Line#4) and *Arabidopsis vih2-3* representing Arabidopsis mutant defective for the expression of AtVIH2 were used. Total AG: arabinogalactan, AX: arabinoxylan and Cellulose (in µg/g) was measured as indicated in Methods. Analyses were made in triplicates with each experimental replicate representing at least five plants for each genotype. Vertical bars represent the standard deviation. # on the bar indicates that the mean is significantly different at $p < 0.01$ (* at $p<0.05$) with respect to their respective control plants.

List of Tables:

Table 1: List of genes identified as an interacting partners of wheat VIH2-3B. The table summarises the information of the predicted gene function (based on the ensemble-BLAST) of the sequenced clones. All the enlist genes resulted in blue colony formation when the screening was performed on the SD-GALα (-AHLT) plates. Respective TRIAE IDs (RefSeq V1.0) are mentioned. Most of these genes show more than once occurrence of the yeast colonies during screening except for S.No 1, 2,3 clones that appeared more than thrice.

S.No	Predicted Biological Annotation	New TRIAE_ ID
1.	*Fasciclin-like arabinogalactan protein (FLA6) (protein ID:* ABI95396.1)	TraesCS2A02G165600
2.	*Glycosyl transferases (GT)*	TraesCS6B02G339100.1
3.	*Xylan arabinosyl transferase (Xat1)*	TraesCS6A02G309400.1
4.	*Glycine-rich cell-wall structural protein-like*	TraesCS2B02G541900
5.	*Alpha-amylase/trypsin inhibitor CM1*	TraesCS7B02G072000
6.	*NADH-ubiquinone reductase complex 1 MLRQ subunit;*	TraesCS7A02G238600
7.	*Hypothetical protein TRIUR3_12806*	TraesCS4A02G016700
8.	*ABC transporter B family member 25 A1-1*	TraesCS5A02G392600

9.	*Short chain dehydrogenase reductase*	TraesCS2B02G116700
10.	*WW domain binding protein (containing PPGPPP motif)*	TraesCS2A02G245500
11.	*Ethylene-responsive element binding protein 1 (EREB1) mRNA, complete cds*	TraesCS7B02G062200
12.	*Triticum aestivum mRNA, clone: tplb0058f16, cultivar Chinese Spring*	TraesCS2A02G558900

1055

1056

1057

Supporting information:

Supplementary Figure 1: Kyte-Doolittle Hydropathy plots for wheat VIH proteins.

Supplementary Figure S2: Expression patterns of *TaVIH* genes' homoeologous in different tissues and stress conditions. RNAseq datasets of (A) Tissues and developmental stages (B) Abiotic (phosphate starvation, heat and drought stress) and (C) Biotic stress conditions were used. The expression values were obtained from expVIP database in the form of TPM values and ratios of stressed to control condition were used to generate heatmaps using MeV software. Green and red colors represent down-regulation and up-regulation of the genes in the specific stresses, as shown by the color bar.

Supplementary Figure S3: Expression of wheat VIH under Pi limiting condition. (A) Positions of phosphate responsive cis-elements in *TaVIH1* and *TaVIH2* gene promoters. The 2 kb promoter sequences of *TaVIH* genes were analysed for the presence of PHO4 binding site and P1BS element. (B) Bar plot depicting fold change levels for all homoeologs of *TaVIH1* and *TaVIH2* in wheat root and shoot tissues upon phosphate deprivation. Expression values were calculated and used to calculate fold change levels from RNA-seq based transcriptomics data (Oono et al., 2013).

Supplementary Figure S4: Western blot analysis, cDNA preparation and screening of the VIH interacting proteins (representative image). (A) Western analysis of c-MYC fused TaVIH1 or TaVIH2 proteins in the yeast strain. (B) Double strand cDNA preparation of

wheat seedling library used for yeast two hybrid interaction studies. The cDNA library was resolved on the 1.2 % agarose gel. Two different cDNA preparations (Rep1 and Rep2) was performed and pooled together for the library preparation. (C) Representative yeast colony map for calculating the mating efficiency (-$LT_{1/1000}$). (D) Representative picture of the yeast colonies with putative interacting clones obtained on the selection plates (-AHLT+αGal). Each of the independent streaked colonies represent single putative interacting clone. Only colonies showing strong-blue coloration were used further for further study.

Supplementary Figure S5: Expression of wheat *Fasciclin-like arabinogalactan protein (FLA6),* TraesCS2A02G165600; g*lycosyl transferases (TaGT),* TraesCS6B02G339100 and *Xylan arabinosyl transferase (TaXat1),* TraesCS6A02G309400. (A) Bar plot depicting fold change levels for *TaFLA6, TaGT* and *TaXat* under drought condition post 1 and 6 hrs of stress. (B) Bar plot depicting fold change levels of wheat *FLA6, TaGT* and *TaXat1* in different wheat tissue (grain, leaf, root, spike and stem). The plots were made using https://wheat.pw.usda.gov/WheatExp/.

Supplementary Figure S6: Flow representation of the preparation and extraction of polysaccharides (Arabinogalactans, Arabinoxylans and Cellulose) form the shoots of *Arabidopsis*

Supplementary Figure S7: GC-MS profiling of arabinogalactans (AG-arabinose+galactose), arabinoxylans (AX-arabinose+xylans) and cellulose in Arabidopsis overexpressing TaVIH2-3B in two independent transgenic lines. Arabidopsis with empty vector (EV) was used as control along with two confirmed homozygous lines referred as Line#4G and Line#5F. (A) Profile indicates for quantification of AG. (B) Profile indicates for quantification of AX and (C) Profile indicates for quantification of cellulose. The lines colour indicates the following: - black: Col-O(EV); red: Line#4G; and green: Line#5F. Inositol (Retention time: 49.2) was used for internal standard while performing GC-MS analysis

Supplementary Figure S8: Expression of *TaVIH* genes in low phytate wheat grains. The expression profiles of both *VIH* genes was studied in seeds of (A) *TaIPK1*-RNAi (Aggarwal et al., 2018) and (B) *TaABCC13*-RNAi transgenic lines (Bhati et al., 2016) and non-transgenic wheat (C-306) as control. cDNA was prepared from DNase treated RNA extracted from 14 DAA seeds of C306, S6-K6-10, S3-D-6-1, S16-D-9-5, S6-K-3-3, K4G3-5-1 and K1B4-2-5 lines. The Ct values were normalised against *TaARF* control. Results indicate mean of three-four technical replicates with standard deviation

Supplementary Table S1: List of *TaVIH* genes with computed physical and chemical parameters. The molecular weight and isoelectric point prediction were done using Expasy ProtParam tool (https://web.expasy.org/protparam/). The sub-cellular localization prediction was done using WoLF PSORT prediction tool (http://www.genscript.com/wolf-psort.html).

Supplementary Table S2: RPKM values of *TaVIH* genes' transcripts for normal (0 day) and phosphate starved (10 day) conditions in root and shoot tissues. The RNAseq data was used from Oono et al., 2014.

Supplementary Table S3: GC-MS analysis in shoot of *Arabidopsis* overexpressing *TaVIH2-3B.* Analysis was done for three biological replicates (independent extractions; Replicate1, Replicate2 and Replicate 3, using 3-4 plants for respective lines). Inositol-derivative was used as an internal control as mentioned in the Methods section. Two independent transgenic lines (Line#4G and Line#5F) along with control plants (Col0-EV) and Arabidopsis mutant *vih2-3* was used for analysis of Arabinogalactans (AG), Arabinoxylans (AX) and cellulose.

Supplementary Table S4: Primers used for this study.

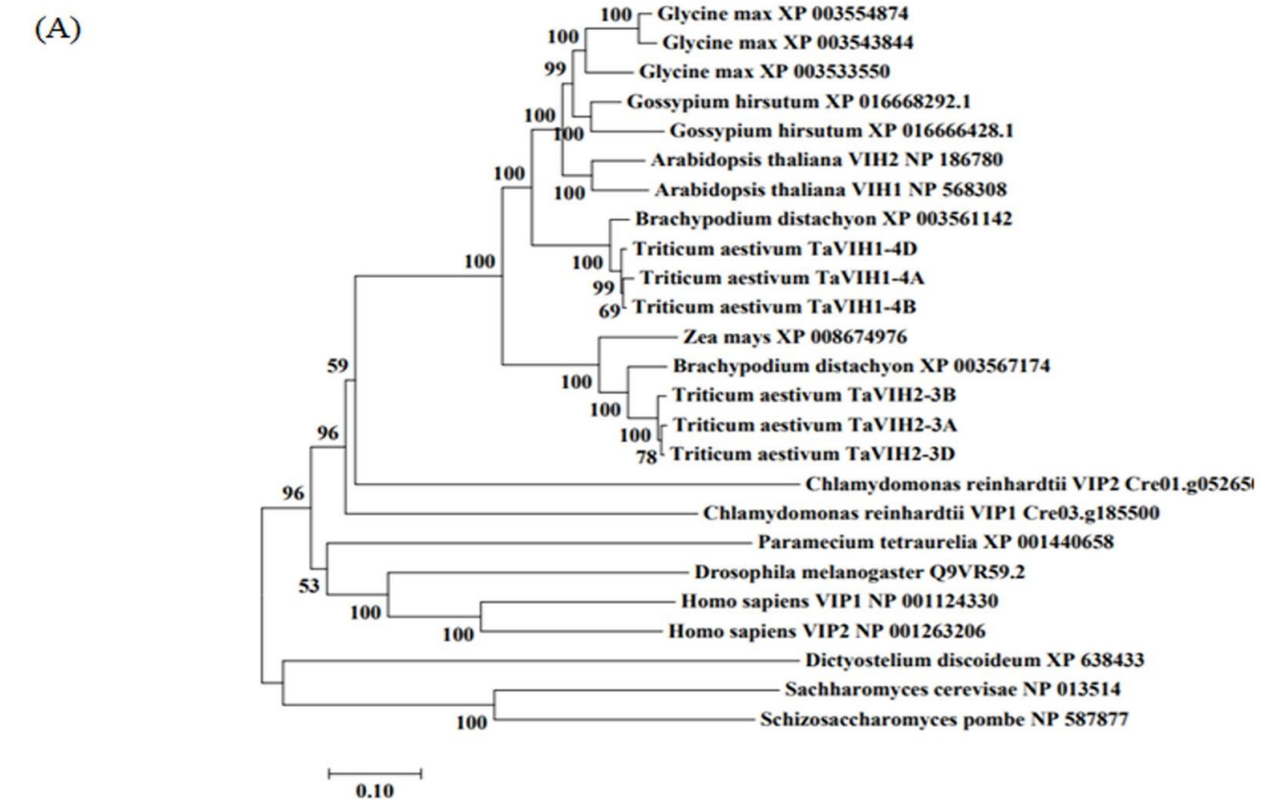

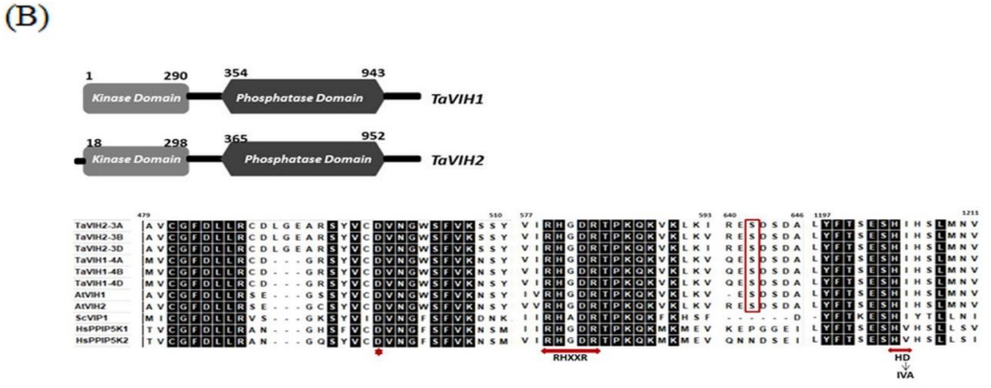

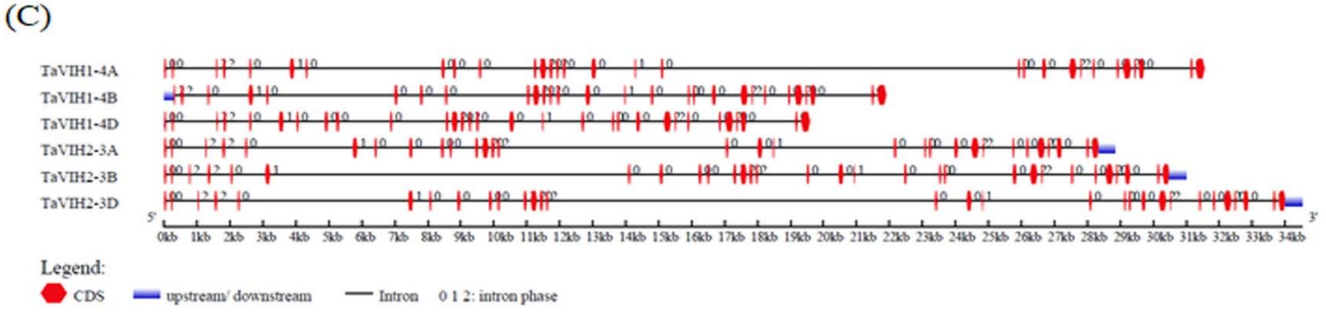

Figure 1

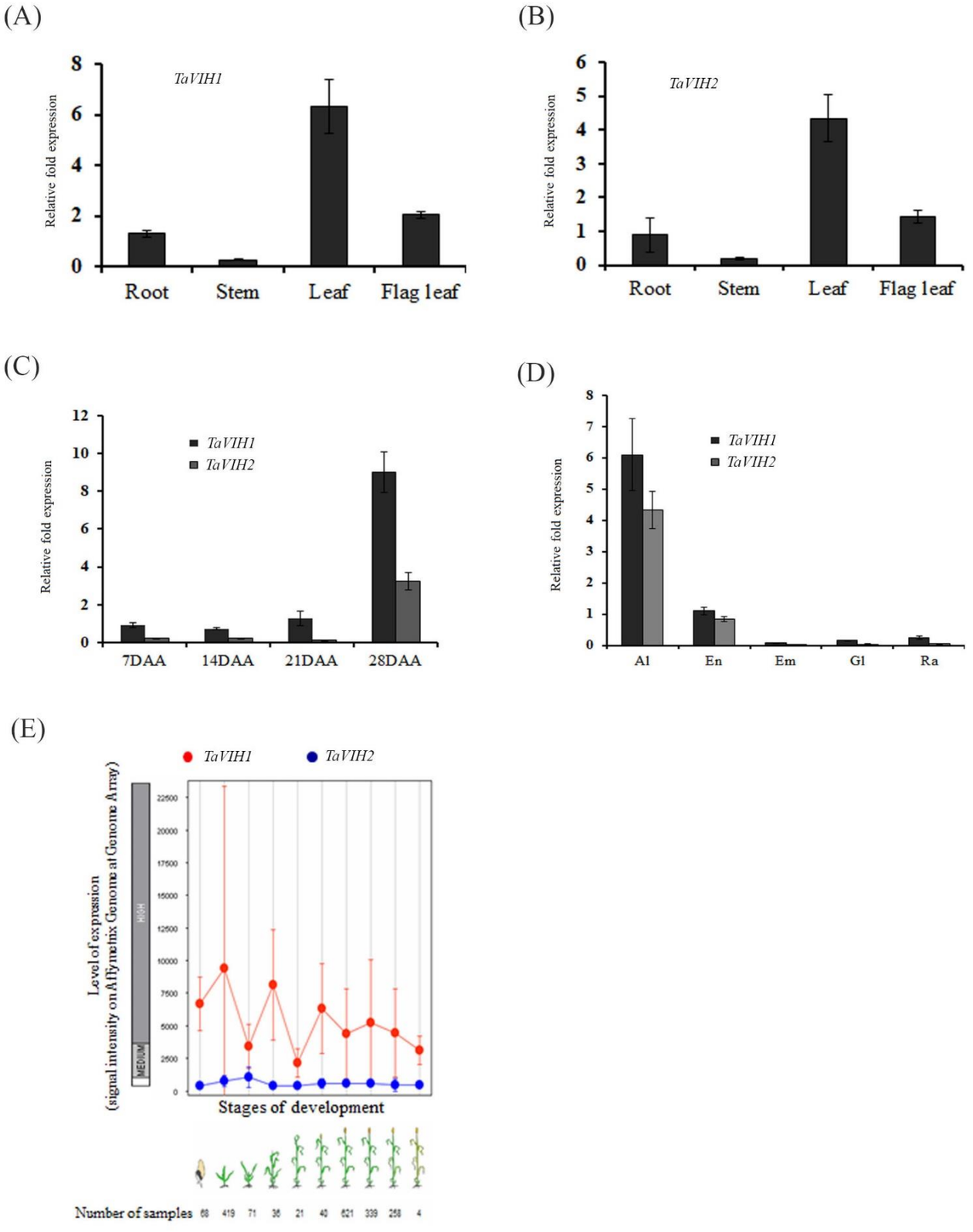

Figure 2

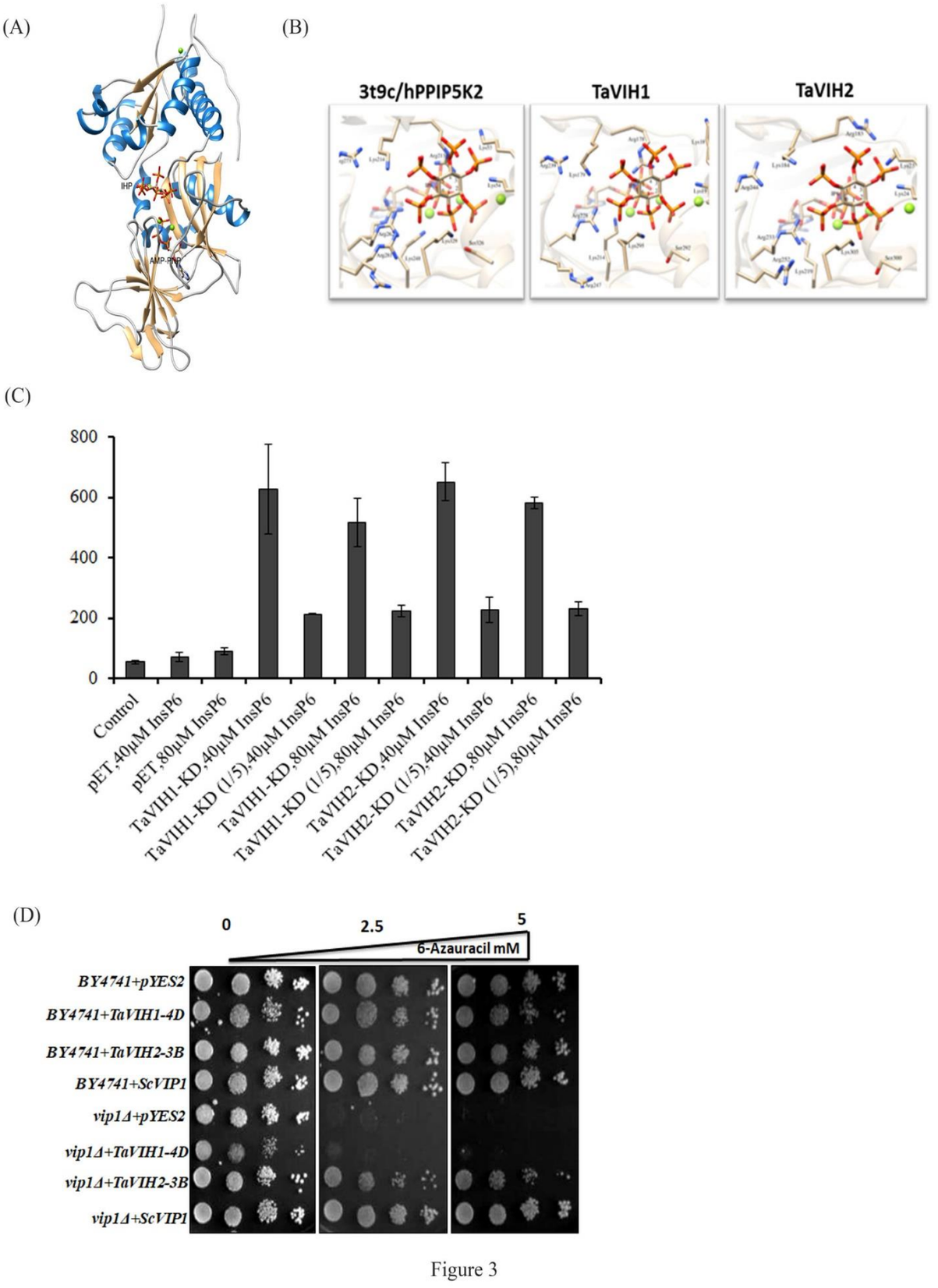

Figure 3

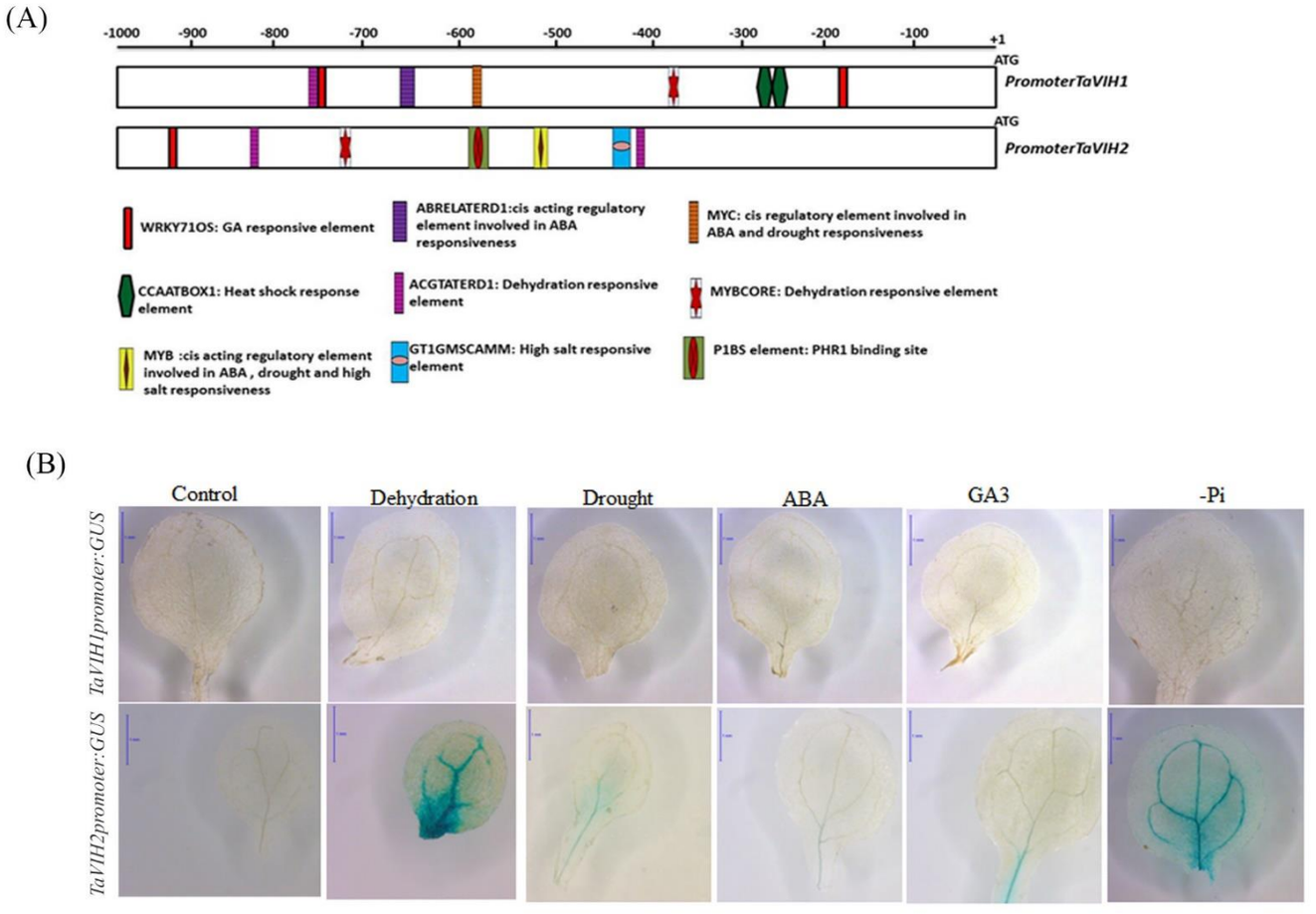

Figure 4

(A)

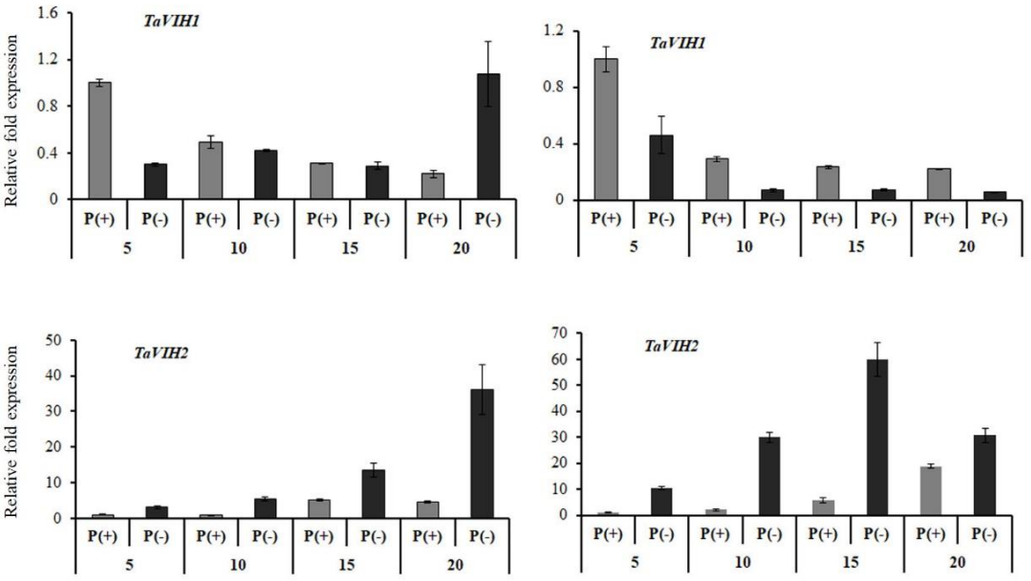

(B)

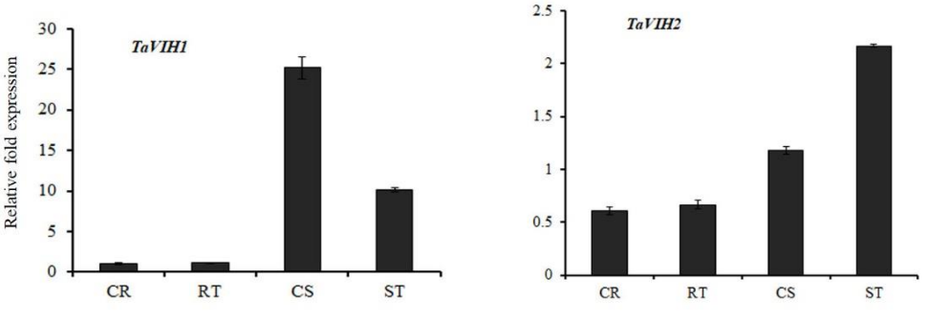

Figure 5

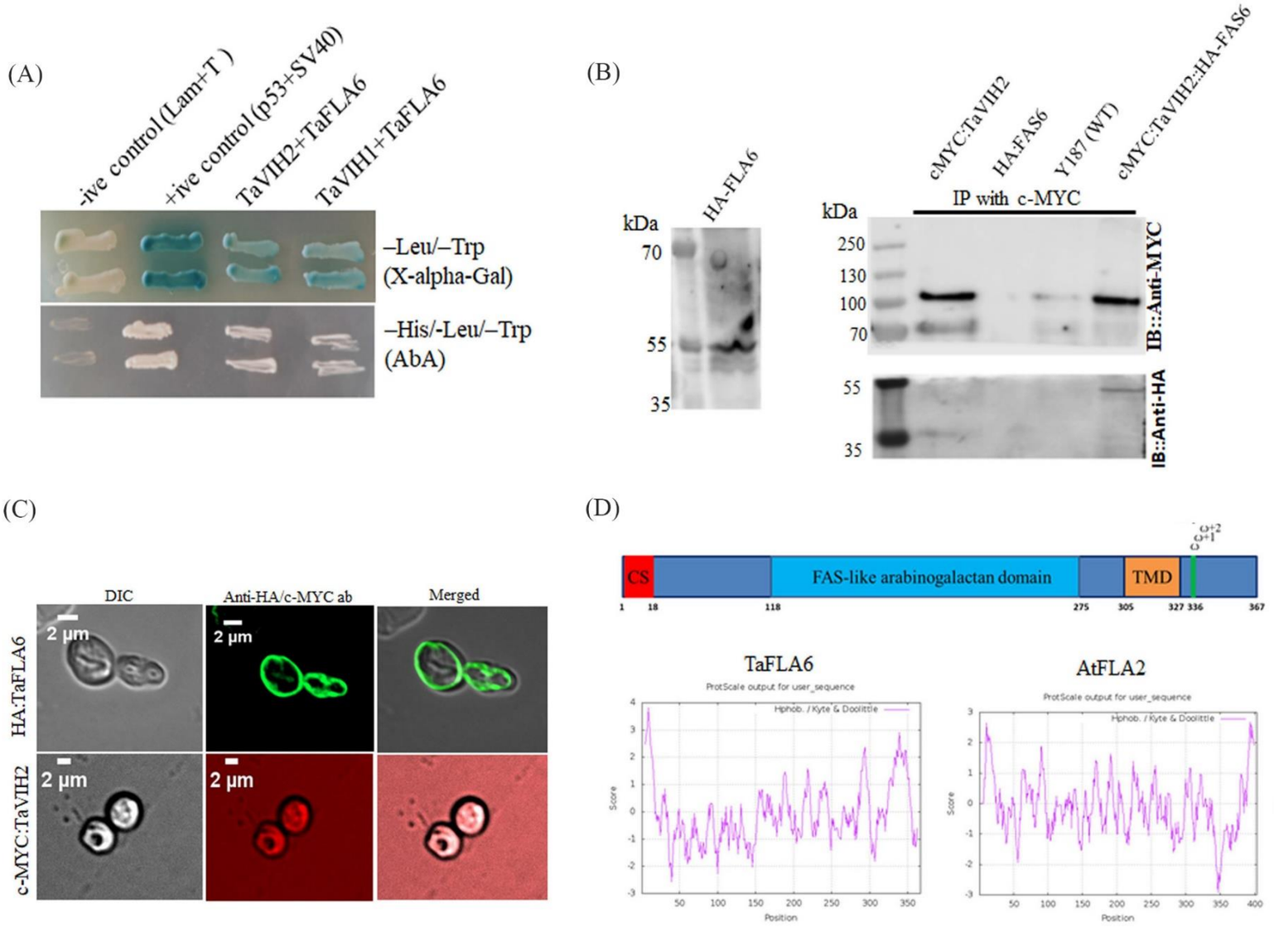

Figure 6

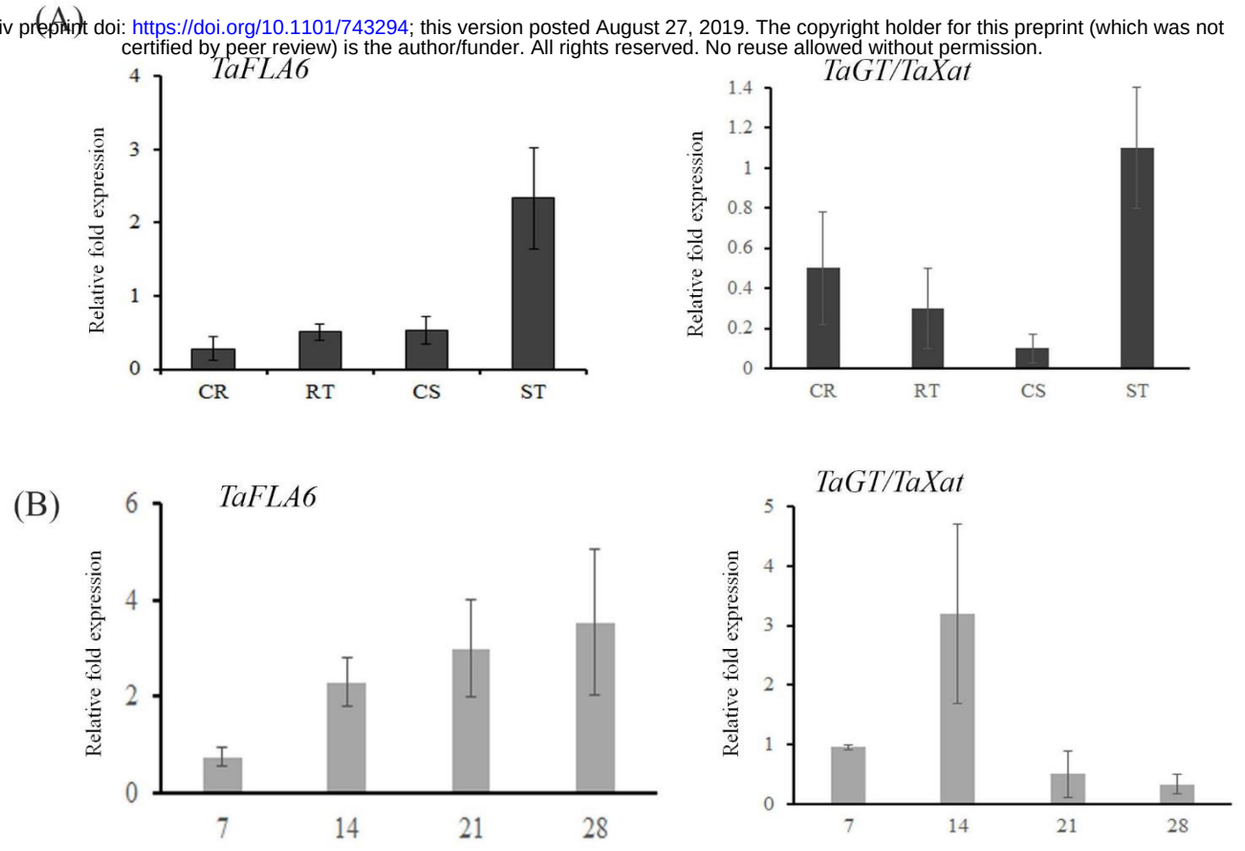

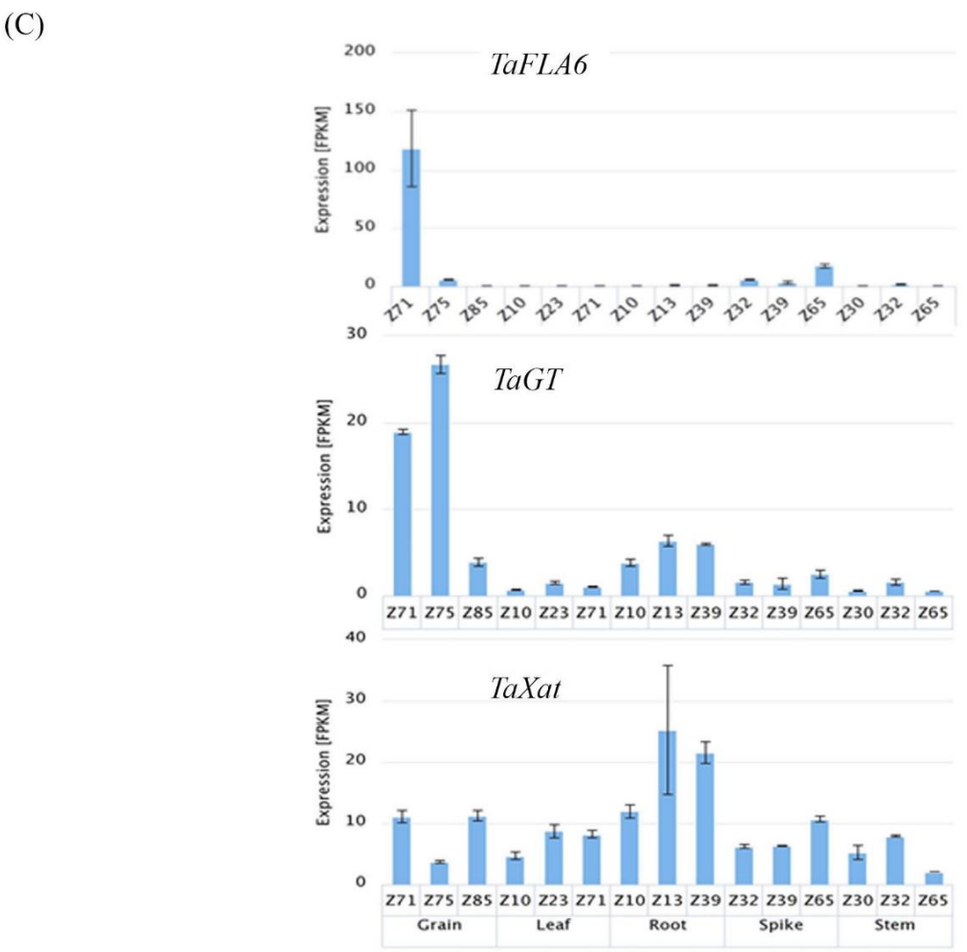

Figure 7

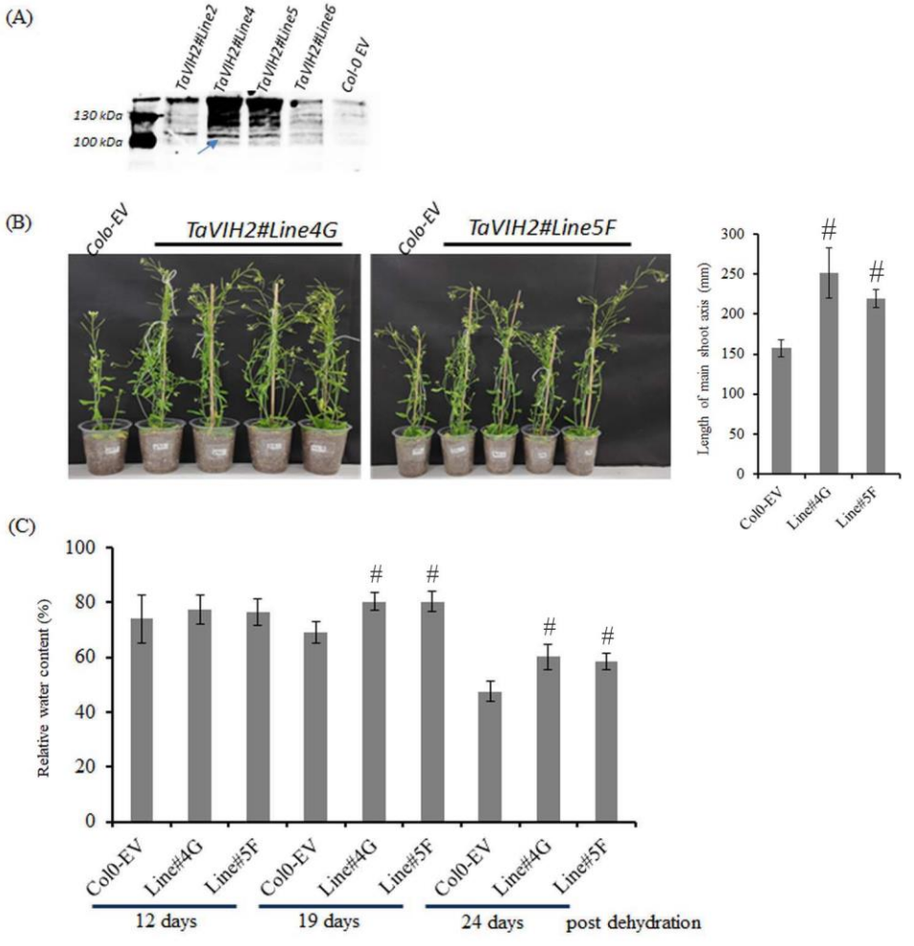

Figure 8

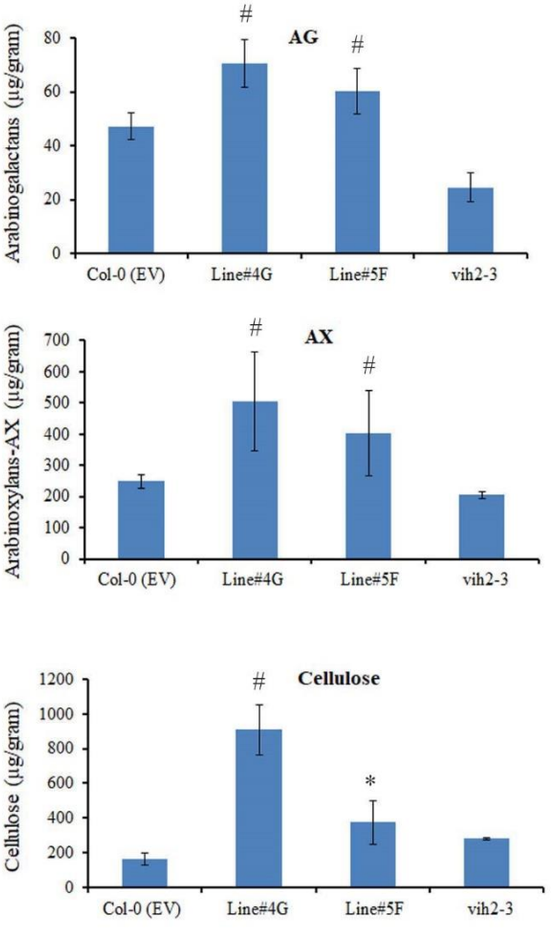

Figure 9